The effects of molecular structure and functional group of rodlike Schiff base mesogen on blue phase stabilization in chiral system

Chiung-Cheng Huang,*[a] Yu-Chang Huang,[a] Wei-Cheng Hsieh,[a] Yen-Jung Chen,[a] Shi-Kai Jiang,[a] Bo-Hao Chen,[b, d] I-Jui Hsu,*[b, c] and Jey-Jau Lee[d]

[a]Department of Chemical Engineering, Tatung University, Taipei 104, Taiwan [a]E-mail:chchhuang@ttu.edu.tw

[a]Tel.: +886-2-77364681

[b]Department of Molecular Science and Engineering, National Taipei University of Technology, Taipei 106, Taiwan

[c] Research and Development Center for Smart Textile Technology, National Taipei University of Technology, Taipei 106, Taiwan

[b,c] E-mail: ijuihsu@mail.ntut.edu.tw

[b,c] Tel.: +886-2-27712171 # 2420

[d]National Synchrotron Radiation Research Center, Hsinchu 300, Taiwan

Electronic supplementary information (ESI)

All of the spectroscopic analysis and microanalytical data for the target products and the intermediates are shown following.

A1. (70 % yield) ^{1}H-NMR ($CDCl_3$): δ (ppm) 10.52 (s, -O**H**, 1H), 10.04 (s, -CH=O, 1H), 8.00 (d, Ar-**H**, 2H, *J* = 8.6 Hz), 7.95 (d, Ar-**H**, 1H, *J* = 8.6 Hz), 7.41 (d, Ar-**H**, 2H, *J* = 8.6 Hz), 6.54 (dd, Ar-**H**, 1H, *J* = 8.9 Hz, *J* = 2.3 Hz), 6.50 (d, Ar-**H**, 1H, *J* = 2.2 Hz), 4.03 (t, -OC**H**$_2$, 2H, *J* = 6.5 Hz), 1.87-1.78 (m, -C**H**$_2$-,2H), 1.51-1.27 (m, -C**H**$_2$-, 6H), 0.92 (t, -C**H**$_3$, 3H, *J* = 6.9 Hz).

A2. (65% yield) ^{1}H-NMR ($CDCl_3$) : δ (ppm) 10.0 (s, -CH=O, 1H), 7.97 (d, Ar-**H**, 2H, *J*=8.5 Hz), 7.86 - 7.82(m, Ar-**H**, 1H), 7.41(d, Ar-**H**, 1H *J*=8.6 Hz), 6.85 - 6.81(m, Ar-**H**, 1H), 4.12 (t, -OC**H$_2$**-, 2H, *J*=6.6 Hz), 1.90 - 1.29 (m, -C**H$_2$**-,-C**H$_3$**, 12H), 0.90 - 0.88 (m, -C**H$_3$**, 3H)

A3. (36 % yield) ^{1}H-NMR ($CDCl_3$): δ (ppm) 11.28 (s, -O**H**, 1H), 10.49 (s, -O**H**, 1H), 9.92 (s, -CH=O, 1H), 7.93 (d, Ar-**H**, 1H, *J* = 8.9 Hz), 7.65 (d, Ar-**H**, 1H, *J* = 8.3 Hz), 6.92 (dd, Ar-**H**, 1H, *J* = 8.3 Hz, *J* = 2.0 Hz), 6.54 (d, Ar-**H**, 1H, *J* = 8.9 Hz), 6.89 (d, Ar-**H**, 1H, *J* = 2.25 Hz), 6.54 (dd, Ar-**H**, 1H, *J* = 8.9 Hz, *J* = 2.6 Hz), 6.50 (d, Ar-**H**, 1H, *J* = 2.3 Hz), 4.03 (t, -OC**H**$_2$, 2H, *J* = 6.5 Hz), 1.81-1.78 (m, -C**H**$_2$-,2H), 1.52-1.24 (m, -C**H**$_2$-, 6H), 0.92 (t, -C**H**$_3$, 3H, *J* = 6.9 Hz).

A4. (41% yield) ^{1}H-NMR ($CDCl_3$) :δ(ppm) 11.2(s, Ar-OH, 1H), 9.90(s, -CH=O, 1H), 7.85 - 7.81 (m, Ar-**H**, 1H), 7.63(d, Ar-**H**, 2H, *J*=8.5 Hz), 6.95 - 6.91(m, Ar-**H**, 2H), 6.85 - 6.82(m, Ar-**H**, 1H), 4.15 (t, -OC**H$_2$**-, 2H, *J*=6.5 Hz), 1.90 - 1.36 (m, -C**H$_2$**-,-C**H$_3$**, 8H), 0.93 (t, -C**H$_3$**, 3H, *J*=6.8 Hz).

H-EI$_6$-OH. ^{1}H-NMR (Acetone-d_6): δ (ppm) 10.59 (s, Ar-O**H**, 1H), 8.68 (s, -C**H**=N-, 1H), 8.08 (d, Ar-**H**, 2H, *J* = 8.7 Hz), 8.03 (d, Ar-**H**, 1H, *J* = 8.9 Hz), 7.47 (d, Ar-**H**, 2H, *J* = 8.6 Hz), 7.31 (d, Ar-**H**, 2H, *J* = 8.8 Hz), 6.99 (d, Ar-**H**, 2H, *J* = 8.9 Hz), 6.64 (dd, Ar-**H**, 1H, *J* = 8.9 Hz, *J* = 2.6 Hz), 6.55 (d, Ar-H, 1H, J = 2.2 Hz), 4.54 - 4.44 (m, -OC**H**, 1H), 4.13 (t, -OC**H$_2$**-, 2H, *J* = 6.5 Hz), 1.87 - 1.29 (m, -C**H$_2$**-,-C**H$_3$**, 21H), 0.94 - 0.87 (m, -C**H$_3$**, 6H). FT-IR (KBr):3430, 2925, 2860, 1678, 1616, 1502, 1250, 1190 cm^{-1}. Elemental analysis for $C_{34}H_{43}NO_5$(percent): calculated C, 74.83, H, 7.94, N, 2.57; found C, 74.83, H, 7.90, N, 2.56.

OH-EI$_6$-OH. ^{1}H-NMR (acetone-d_6): δ (ppm) 13.81 (s, Ar-O**H**, 1H), 10.56 (s, Ar-O**H**, 1H), 8.94 (s, -C**H**=N-, 1H), 8.00 (d, Ar-**H**, 1H, *J* = 8.9 Hz), 7.66 (d, Ar-**H**, 1H, *J* = 9.3 Hz), 7.42 (d, Ar-**H**, 2H, *J* = 8.9 Hz), 7.02 (d, Ar-**H**, 2H, *J* = 8.9 Hz), 6.93 – 6.92 (m, Ar-**H**, 2H), 6.62 (dd, Ar-**H**, 1H, *J* = 9.0 Hz, *J* = 2.3 Hz), 6.54 (d, Ar-H, 1H, *J* = 2.3 Hz), 4.57 - 4.47 (m, -OC**H**, 1H), 4.12 (t, -OC**H$_2$**-, 2H, *J* = 6.5 Hz), 1.84 - 1.30 (m, -C**H$_2$**-,-

C**H$_3$**, 21H), 0.93 - 0.90 (m, -C**H$_3$**, 6H). FT-IR (KBr): 3232, 2924, 2856, 1684, 1616, 1506 , 1250, 1157 cm^{-1}. Elemental analysis for $C_{34}H_{43}NO_6$ (percent): calculated C, 72.70, H, 7.72, N, 2.49; found C, 72.82, H, 7.74, N, 2.49.

H-EI$_6$-F. ^{1}H-NMR ($CDCl_3$): δ (ppm) 8.50 (s, -C**H**=N-, 1H), 7.96 (d, Ar-**H**, 2H, *J*=8.6 Hz), 7.86 (m, Ar-**H**, 1H), 7.34 (d, Ar-**H**, 2H, *J*=8.6 Hz), 7.23 (d, Ar-**H**, 2H, *J*=8.7 Hz), 6.92 (d, Ar-**H**, 2H, *J*=8.7Hz), 6.84-6.80 (m, Ar-**H**, 1H), 4.38 - 4.35 (m, -OC**H**, 1H), 4.15 (t, -OC**H$_2$**-, 2H, *J*=6.6 Hz), 1.90 - 1.31 (m, -C**H$_2$**-,-C**H$_3$**, 21H), 0.95 - 0.88 (m, -C**H$_3$**, 6H). FT-IR (KBr): 2917, 2854, 1737, 1617, 1506, 1282, 1197,1076 cm^{-1}. Elemental analysis for $C_{34}H_{41}F_2NO_4$ (percent): calculated C, 72.19, H, 7.31, N, 2.48; found C, 71.31, H, 7.43, N, 2.20.

OH-EI$_6$-F. ^{1}H-NMR ($CDCl_3$): δ (ppm) 13.8 (s, Ar-OH, 1H) 8.63 (s, -C**H**=N-, 1H), 7.84 (m, Ar-**H**, 1H), 7.42 (d, Ar-**H**, 1H, *J*=8.4 Hz), 7.28 - 7.26 (d, Ar-**H**, 2H), 6.94 (d, Ar-**H**, 2H, *J*=8.8 Hz), 6.90(d, Ar-**H**, 1H, *J*=2.2 Hz), 6.85 - 6.82 (m, Ar-**H**, 2H), 4.41 - 4.35 (m, -OC**H**, 1H), 4.15 (t, -OC**H$_2$**-, 2H, *J*=6.6 Hz), 1.91 -1.30 (m, -C**H$_2$**-,-C**H$_3$**, 21H), 0.95 - 0.88 (m, -C**H$_3$**, 6H). FT-IR (KBr): 2919, 2854, 1731, 1616, 1509, 1255, 1195, 1078 cm^{-1}. Elemental analysis for $C_{34}H_{41}F_2NO_5$ (percent): calculated C, 70.20, H, 7.10, N, 2.41; found C, 70.39, H, 7.28, N, 2.16.

B1. ^{1}H-NMR ($CDCl_3$): δ (ppm) 8.33 (d, Ar-**H**, 2H, *J* = 9.3 Hz), 8.14 (d, Ar-**H**, 2H, *J* = 8.9 Hz), 7.41 (d, Ar-**H**, 2H, *J* = 9.3 Hz), 7.00 (d, Ar-**H**, 2H, *J* = 9.0 Hz), 4.07 (t, -OC**H$_2$**, 2H, *J* =6.6 Hz), 1.88-1.79 (m, -C**H$_2$**-, 2H), 153-1.34 (m, -C**H$_2$**-, 6H), 0.93 (t, -CH_3, 3**H**, *J* = 7.4 Hz).

B2. ^{1}H-NMR ($CDCl_3$): δ (ppm) 10.42 (s, -O**H**, 1H), 8.35 (d, Ar-**H**, 2H, *J* = 9.3 Hz), 7.94 (d, Ar-**H**, 1H, *J* = 8.9 Hz), 7.42 (d, Ar-**H**, 2H, *J* = 9.0 Hz), 6.55 (dd, Ar-**H**, 1H, *J* = 2.6 Hz, *J* = 8.9 Hz), 6.51 (d, Ar-**H**, 1H, *J* = 2.6 Hz), 4.03 (t, -OC**H$_2$**, 2H, *J* = 6.5 Hz), 1.87-1.77 (m, -C**H$_2$**-, 2H), 1.51-1.34 (m, -C**H$_2$**-, 6H), 0.93 (t, -C**H$_3$**, 3H, *J* = 7.1 Hz).

B3.^{1}H-NMR ($CDCl_3$): δ (ppm) 8.34 (d, Ar-**H**, 2H, *J* = 9.3 Hz), 7.89-7.83 (m, Ar-**H**, 1H), 7.44 (d, Ar-**H**, 2H, *J* = 9.3 Hz), 6.89-6.83 (m, Ar-**H**, 1H), 4.18-4.10 (m, -OC**H$_2$**, 2H), 1.94-1.85 (m, -C**H$_2$**-, 8H), 0.93 (t, -C**H$_3$**, 3H, *J* = 7.0 Hz).

C1.[1]H-NMR ($CDCl_3$): δ (ppm) 8.13 (d, Ar-**H**, 2H, J = 9.2 Hz), 6.98 (t, Ar-**H**, 4H, J = 8.7 Hz), 6.72 (d, Ar-H, 2**H**, J = 8.8 Hz), 4.04 (t, -OC**H**$_2$, 2H, J = 6.6 Hz), 1.87-1.78 (m, -C**H**$_2$-, 2H), 1.53-1.26 (m, -C**H**$_2$-, 6H), 0.92 (t, -C**H**$_3$, 3H, J = 7.0 Hz).

C2. [1]H-NMR ($CDCl_3$): δ (ppm) 10.80 (d, -O**H**, 1H, J = 11.6 Hz), 7.94 (d, Ar-**H**, 1H, J = 8.7 Hz), 7.00-6.96 (m, Ar-**H**, 2H), 6.72 (d, Ar-**H**, 1H, J = 8.9 Hz), 6.61 (d, Ar-**H**, 1H, J = 8.9 Hz), 6.52-6.47 (m, Ar-**H**, 2H), 4.01 (t, -OC**H**$_2$, 2H, J = 6.6 Hz), 1.85-1.76 (m, -C**H**$_2$-, 2H), 1.52-1.32 (m, -C**H**$_2$-, 6H), 0.92 (t, -C**H**$_3$, 3H, J = 7.0 Hz).

C3. [1]H-NMR ($CDCl_3$): δ (ppm) 7.85-7.79 (m, Ar-**H**, 1H), 7.00 (d, Ar-**H**, 2H, J = 8.6 Hz), 6.84-6.78 (m, Ar-**H**, 1H), 6.71 (d, Ar-**H**, 2H, J = 8.6 Hz), 4.15-4.07 (m, -OC**H**$_2$,2H), 1.91-1.26 (m, -C**H**$_2$-, 8H), 0.92 (t, -C**H**$_3$, 3H, J = 7.0 Hz).

D1.[1]H-NMR ($CDCl_3$): δ (ppm) 9.87 (s, Ar-C**H**O, 1H), 7.82 (d, Ar-**H**, 2H, J = 8.9 Hz), 6.97 (d, Ar-**H**, 2H, J = 8.9 Hz), 4.49 (m, -OC**H**, 1H), 1.83-1.18 (m, -C**H**$_2$-, -C**H**$_3$, 13H), 0.88 (t, -C**H**$_3$, 3H, J = 6.8 Hz).

D2.[1]H-NMR ($CDCl_3$): [1]H-NMR ($CDCl_3$): δ (ppm) 11.49 (s, Ar-O**H**, 1H), 9.70 (s, Ar-C**HO**, 1H), 7.42 (d, Ar-**H**, 2H, J = 8.9 Hz), 6.51 (dd, Ar-**H**, 2H, J = 8.9 Hz, J = 2.2 Hz), 4.48 (m, -OC**H**, 1H), 1.82-1.20 (m, -C**H**$_2$-, -C**H**$_3$, 13H), 0.89 (t, -C**H**$_3$, 3H, J = 7.0 Hz).

H-EIII$_6$. [1]H-NMR ($CDCl_3$): δ (ppm) 8.40 (s, -C**H**=N-, 1H), 7.84 (d, Ar-**H**, 2H, J = 8.6 Hz), 7.23 (d, Ar-**H**, 4H, J = 3.4 Hz), 6.98 (dd, Ar-**H**, 4H, J = 8.6 Hz, J = 5.2 Hz), 4.51-4.42 (m, -OC**H**, 1H), 4.06 (t, -OC**H**$_2$, 2H, J = 6.6 Hz), 1.88-1.26 (m, -C**H**$_2$-, -C**H**$_3$, 21H), 0.95-0.84 (m, -C**H**$_3$, 6H). FT-IR (KBr): 2925, 2857, 1725, 1604, 1567, 1504, 1245, 1159, 1056 cm^{-1}. Elemental analysis for $C_{34}H_{43}NO_4$ (percent): calculated C, 77.09, H, 8.18, N, 2.64; found C, 77.23, H, 8.32, N, 2.46.

OH-EIII$_6$. [1]H-NMR (Acetone-d_6): δ (ppm) 13.47 (s, -O**H**, 1H), 8.83 (d, -C**H**=N-, 1H, J = 2.4 Hz), 8.13 (d, Ar-**H**, 2H, J = 8.9 Hz), 7.46 (d, Ar-**H**, 3H, J = 9.1 Hz), 7.33 (d, Ar-**H**, 2H, J = 9.0 Hz), 7.11 (d, Ar-**H**, 2H, J = 8.9 Hz), 6.56 (dd, Ar-**H**, 1H, J = 8.7 Hz, J = 2.6 Hz), 6.47 (d, Ar-**H**, 1H, J = 2.3 Hz), 4.63 -4.53 (m, -OC**H**, 1H), 4.14 (t, -OC**H**$_2$, 2H, J = 6.5 Hz), 1.88-1.30 (m, -C**H**$_2$-, -C**H**$_3$, 21H), 0.94-0.86 (m, -C**H**$_3$, 6H). FT-IR (KBr): 3741, 2919, 2856, 1720, 1614, 1506, 1259, 1174 cm^{-1}. Elemental analysis for $C_{34}H_{43}NO_5$ (percent): calculated C, 74.83, H, 7.94, N, 2.57; found C, 74.82, H, 7.91, N, 2.55.

H-EIII$_6$-OH. ^{1}H-NMR (Acetone-d_6): δ (ppm) 10.67 (s, -O**H**, 1H), 8.56 (d, -C**H**=N-, 1H), 8.02 (d, Ar-**H**, 2H, J = 8.9 Hz), 7.92 (d, Ar-**H**, 2H, J = 8.9 Hz), 7.34 (s, Ar-**H**, 4H), 7.07 (d, Ar-**H**, 2H, J = 8.9 Hz), 6.63 (dd, Ar-**H**, 1H, J = 8.9 Hz, J = 2.3 Hz), 6.54 (d, Ar-**H**, 1H, J = 2.5 Hz), 4.67 -4.56 (m, -OC**H**, 1H), 4.12 (t, -OC**H**$_2$, 2H, J = 6.5 Hz), 1.87-1.31 (m, -C**H**$_2$-, -C**H**$_3$, 21H), 0.94-0.86 (m, -C**H**$_3$, 6H). FT-IR (KBr): 3739, 2927, 2858, 1671, 1617, 1504, 1254, 1192 cm^{-1}. Elemental analysis for $C_{34}H_{43}NO_5$ (percent): calculated C, 74.83, H, 7.94, N, 2.57; found C, 74.64, H, 7.97, N, 2.53.

OH-EIII$_6$-OH.^{1}H-NMR (Acetone-d_6): δ (ppm) 13.41 (s, -O**H**, 1H), 10.61 (s, -O**H**, 1H), 8.82 (d,-C**H**=N-, 1H, J = 2.9 Hz), 8.00 (d, Ar-**H**, 1H, J = 8.9 Hz), 7.48-7.46 (m, Ar-**H**, 3H), 7.37 (d, Ar-**H**, 2H, J = 8.9 Hz), 6.61 (dd, Ar-**H**, 1H, J = 9.1 Hz, J = 2.4 Hz), 6.55-6.53 (m, Ar-**H**, 2H), 6.46 (d, Ar-H, 1H, J = 2.3 Hz), 4.59-4.55 (m, -OC**H**, 1H), 4.11 (t, -OC**H**$_2$, 2H, J = 6.5 Hz), 1.83-1.31 (m, -C**H**$_2$-, -C**H**$_3$, 21H), 0.92-0.87 (m, -C**H**$_3$, 6H). FT-IR (KBr): 3469, 2921, 2857, 1672, 1623, 1509, 1261, 1186 cm^{-1}. Elemental analysis for $C_{34}H_{43}NO_6$ (percent): calculated C, 72.70, H, 7.72, N, 2.49; found C, 72.81, H, 7.89, N, 2.39.

H-EIII$_6$-F. ^{1}H-NMR (Acetone-d_6): δ (ppm) 8.55 (s, -C**H**=N-, 1H), 7.92 (d, Ar-**H**, 3H, J = 8.8 Hz), 7.36-7.29 (m, Ar-**H**, 4H), 7.23-7.17 (m, Ar-**H**, 1H), 7.07 (d, Ar-**H**, 2H, J = 8.9 Hz), 4.66-4.56 (m, -OC**H**, 1H), 4.29 (t, -OC**H**$_2$, 2H, J = 6.5 Hz), 1.93-1.30 (m, -C**H**$_2$-, -C**H**$_3$, 21H), 0.95-0.87 (m, -C**H**$_3$, 6H). FT-IR (KBr): 2927, 2857, 1735, 1617, 1509, 1471, 1251, 1243 cm^{-1}. Elemental analysis for $C_{34}H_{41}F_2NO_4$ (percent): calculated C, 72.19, H, 7.31, N, 2.48; found C, 72.07, H, 7.49, N, 2.35.

OH-EIII$_6$-F. ^{1}H-NMR (Acetone-d_6): δ (ppm) 13.46 (s, -O**H**, 1H), 8.84 (d, -C**H**=N-, 1H, J = 2.6 Hz), 7.97-7.90 (m, Ar-**H**, 1H), 7.51-7.46 (m, Ar-**H**, 3H), 7.37 (d, Ar-**H**, 2H, J = 8.9 Hz), 7.23-7.17 (m, Ar-**H**, 1H), 6.56 (dd, Ar-**H**, 1H, J = 8.5 Hz, J = 2.5 Hz), 6.48 (d, Ar-**H**, 1H, J = 2.6 Hz), 4.64 -4.54 (m, -OC**H**, 1H), 4.29 (t, -OC**H**$_2$, 2H, J = 6.5 Hz), 1.93-1.29 (m, -C**H**$_2$-, -C**H**$_3$, 21H), 0.94-0.87 (m, -C**H**$_3$, 6H). FT-IR (KBr): 3448, 2929, 2861, 1722, 1625, 1511, 1251, 1178 cm^{-1}. Elemental analysis for $C_{34}H_{41}F_2NO_5$ (percent): calculated C, 70.20, H, 7.10, N, 2.41; found C, 70.03, H, 7.18, N, 2.32.

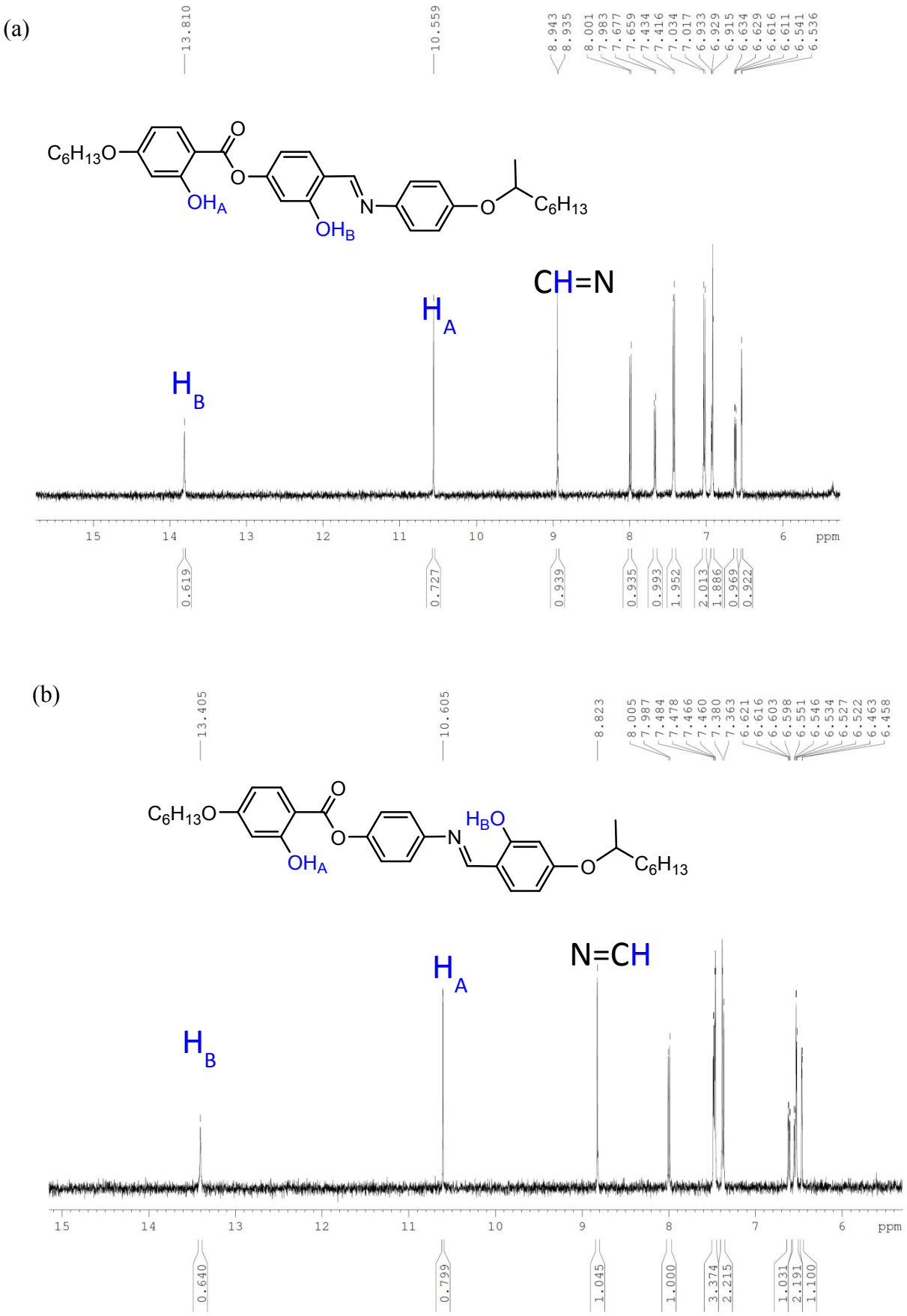

Figure S1 The ^{1}H NMR spectra of Schiff base compounds **OH-EI$_6$-OH** (a) and **OH-EIII$_6$-OH** (b) in the range of 6-15 ppm

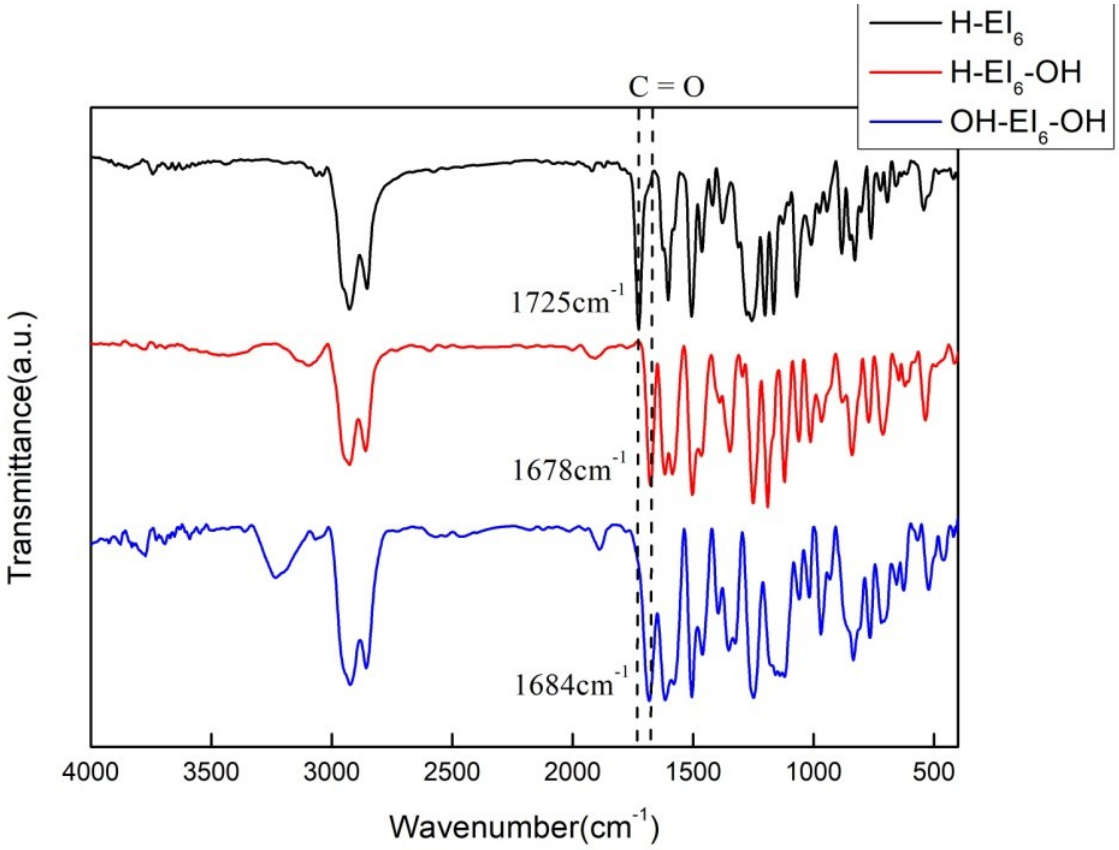

Figure S2 FT-IR spectra of Schiff base compounds **H-EI$_6$**, **H-EI$_6$-OH** and **OH-EI$_6$-OH**

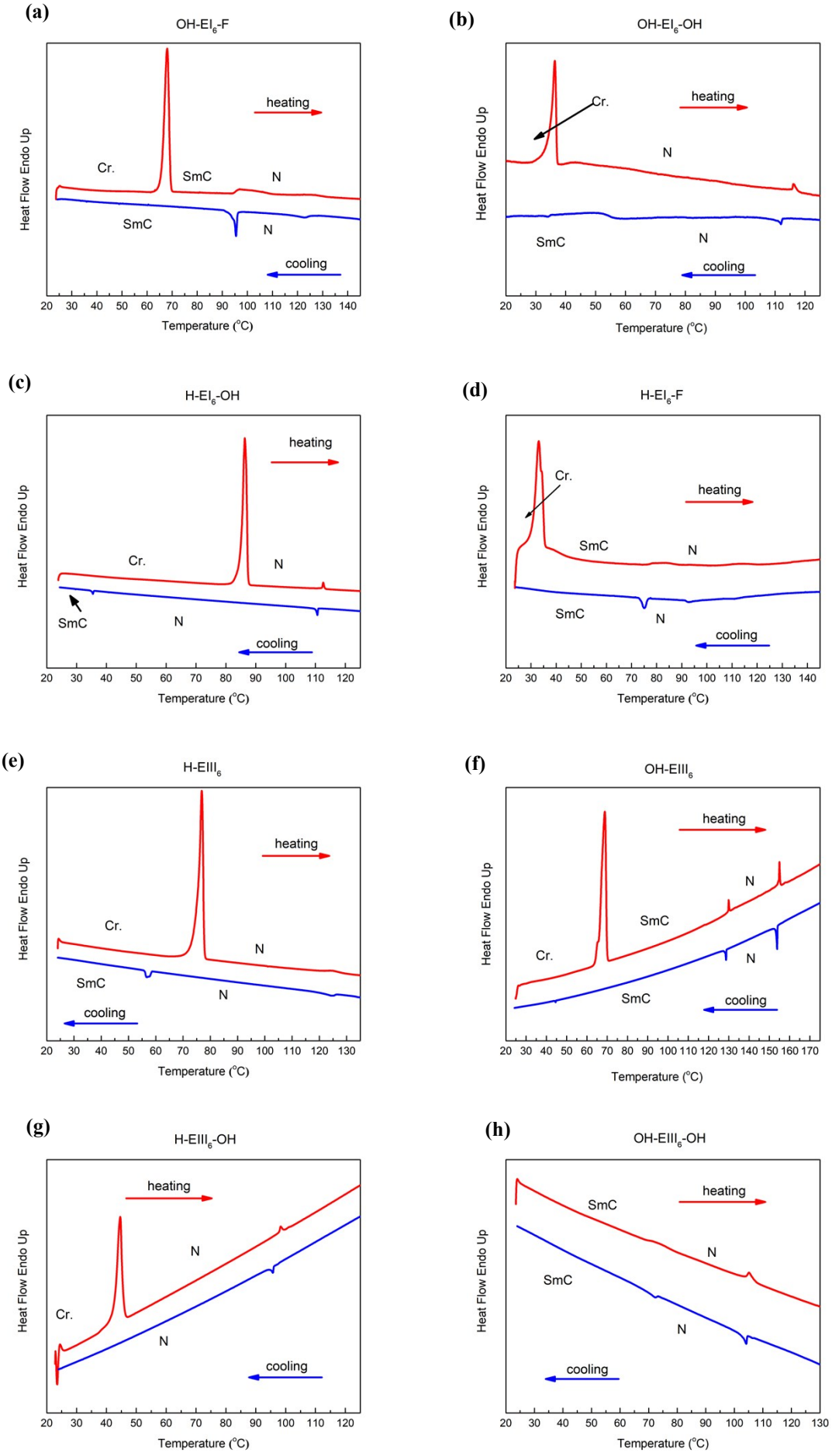
(a)
OH-EI6-F
heating
Cr.
SmC
N
SmC
N
cooling
Heat Flow Endo Up
Temperature (°C)
(b)
OH-EI6-OH
Cr.
heating
N
SmC
N
cooling
Heat Flow Endo Up
Temperature (°C)
(c)
H-EI6-OH
heating
Cr.
N
SmC
N
cooling
Heat Flow Endo Up
Temperature (°C)
(d)
H-EI6-F
Cr.
heating
SmC
N
SmC
N
cooling
Heat Flow Endo Up
Temperature (°C)
(e)
H-EIII6
heating
Cr.
N
SmC
N
cooling
Heat Flow Endo Up
Temperature (°C)
(f)
OH-EIII6
heating
N
SmC
Cr.
N
SmC
cooling
Heat Flow Endo Up
Temperature (°C)
(g)
H-EIII6-OH
heating
N
Cr.
N
cooling
Heat Flow Endo Up
Temperature (°C)
(h)
OH-EIII6-OH
SmC
heating
N
SmC
N
cooling
Heat Flow Endo Up
Temperature (°C)

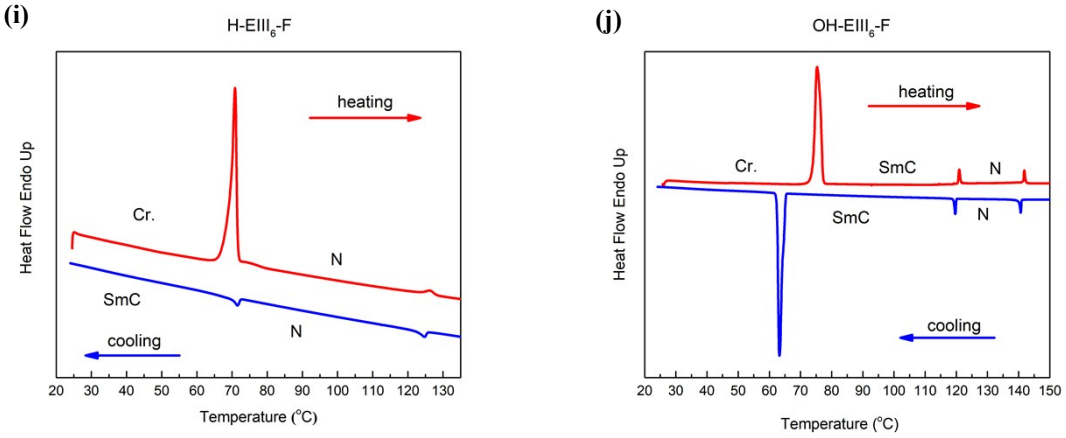

Figure S3 The DSC measurements of all racemic Schiff base mesogens on heating and cooling recycle.

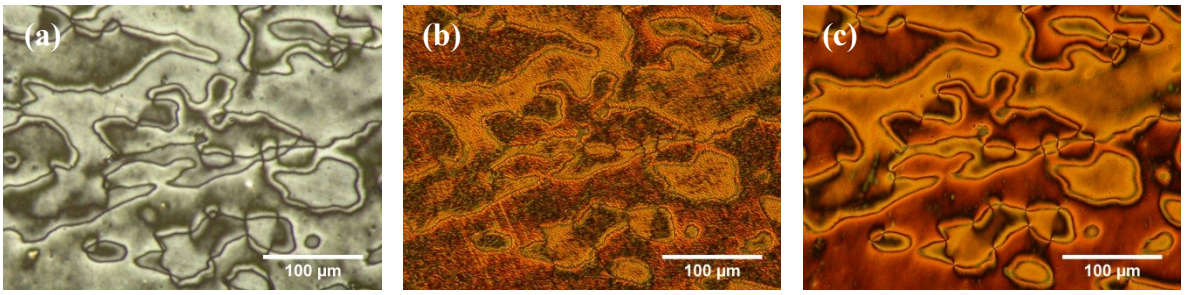

Figure S4 Microphotographs for compound **H-EI$_6$-OH** : (a) N texture at 109.0°C; (b) N-SmC texture at 37.2°C; (c) SmC texture at 36.0°C.

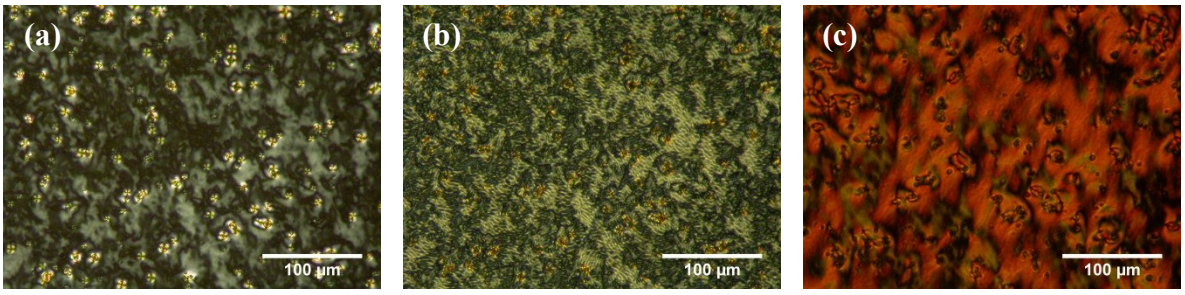

Figure S5 Microphotographs for compound **OH-EIII$_6$-OH** : (a) N texture at 99.6°C; (b) N-SmC texture at 78.5°C; (c) SmC texture at 30.0°C.

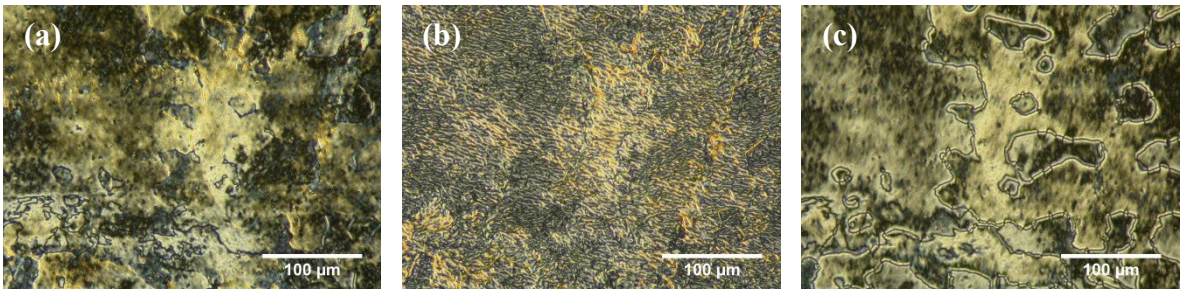

Figure S6 Microphotographs for compound **OH-EIII$_6$-F** : (a) N texture at 129.7°C; (b) N-SmC texture at 108.2°C; (c) SmC texture at 59.6°C.

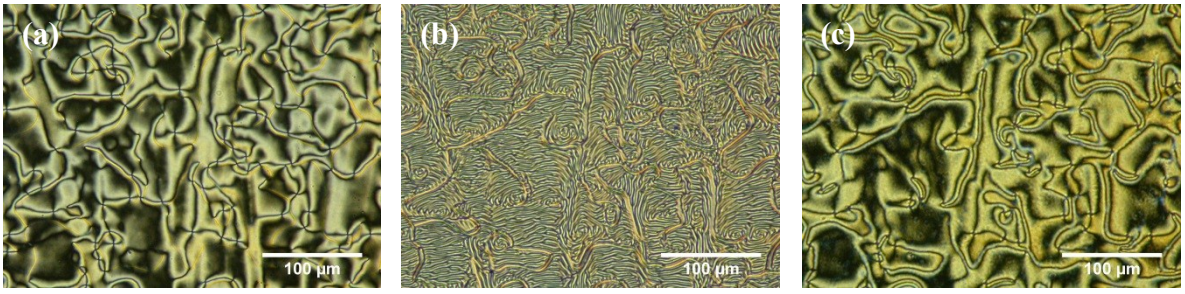

Figure S7 Microphotographs for compound **H-EIII$_6$-F** : (a) N texture at 99.6°C; (b) N-SmC texture at 78.5°C; (c) SmC texture at 36.0°C.

H-EI$_6$-OH T = RT

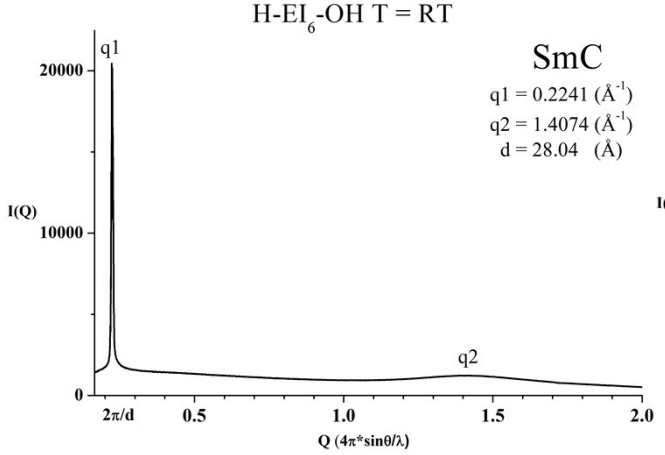

H-EI$_6$-OH RT after 20mins

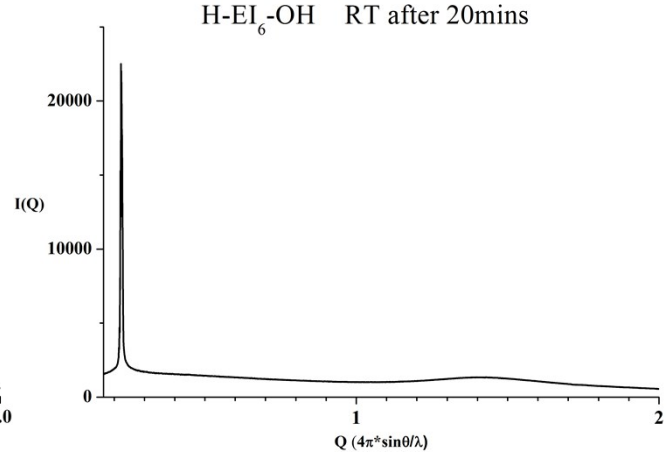

H-EI$_6$-F T = 51°C

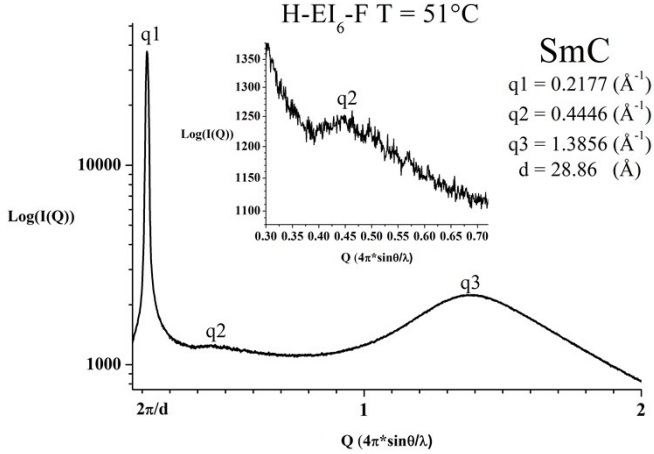

H-EI$_6$-F T = RT

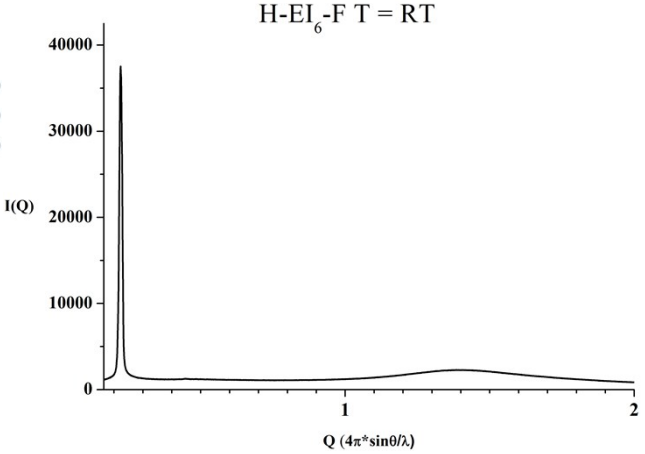

OH-EI$_6$-OH

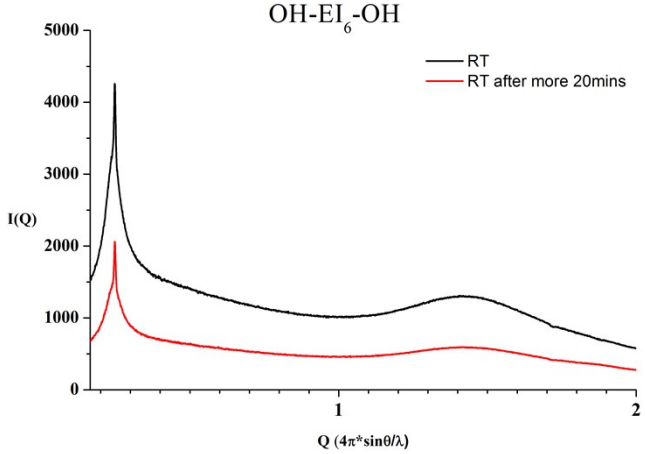

OH-EI$_6$-F T = 61°C

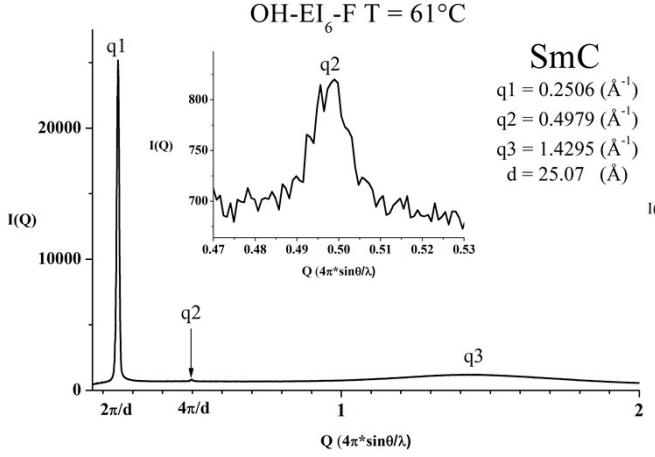

OH-EI$_6$-F T = RT

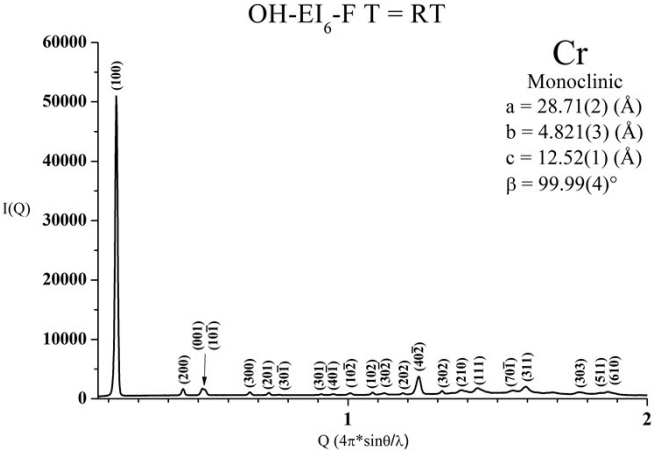

H-EIII$_6$ T = 42°C

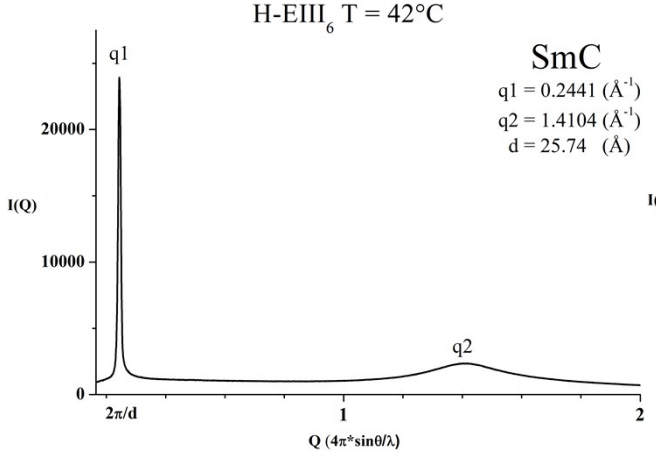

H-EIII$_6$ T = RT

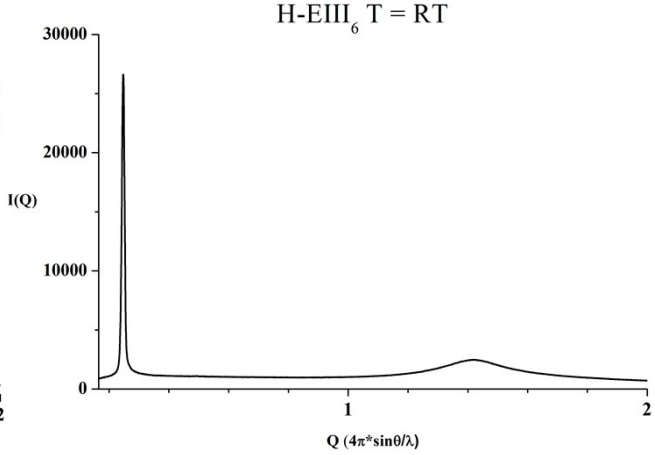

OH-EIII$_6$ T = 77°C

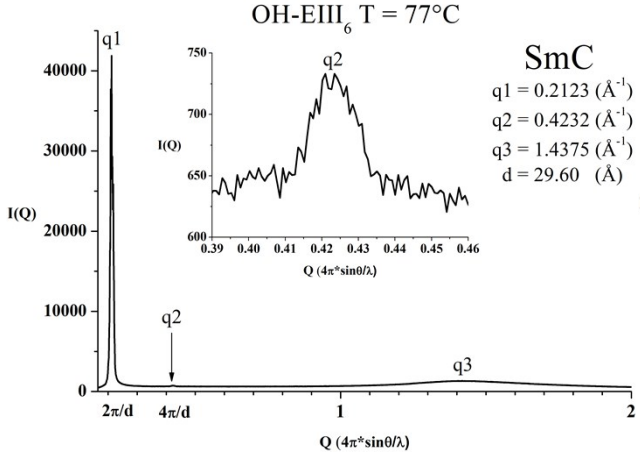

OH-EIII$_6$ T = RT

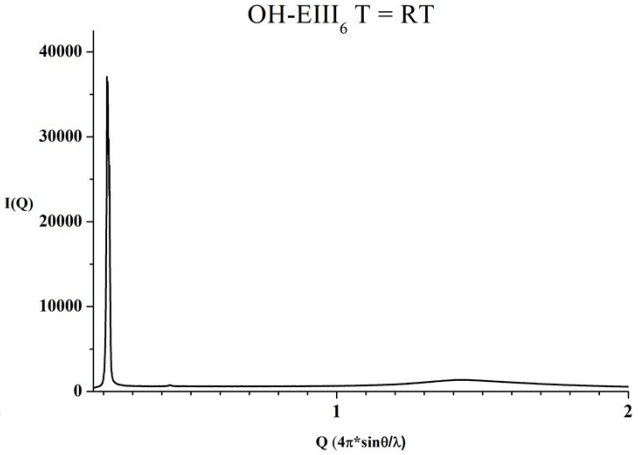

H-EIII$_6$-F T = 50°C

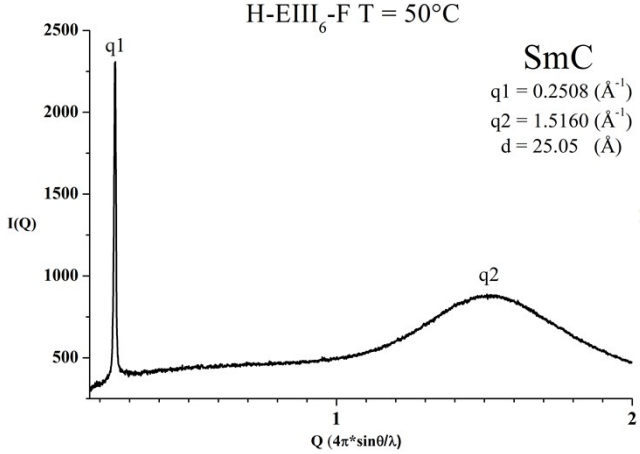

H-EIII$_6$-F T = RT

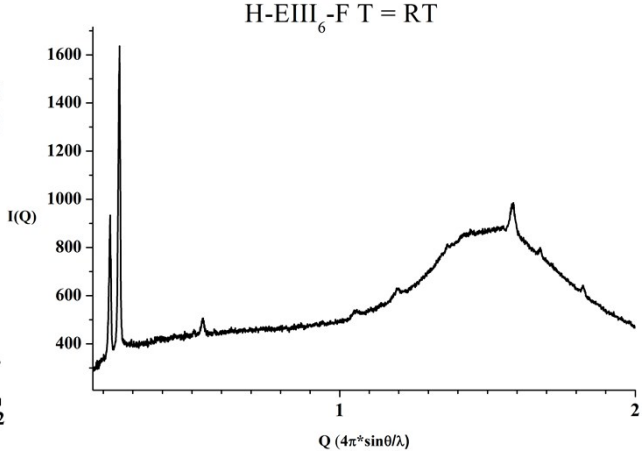

OH-EIII$_6$-OH T = 49°C

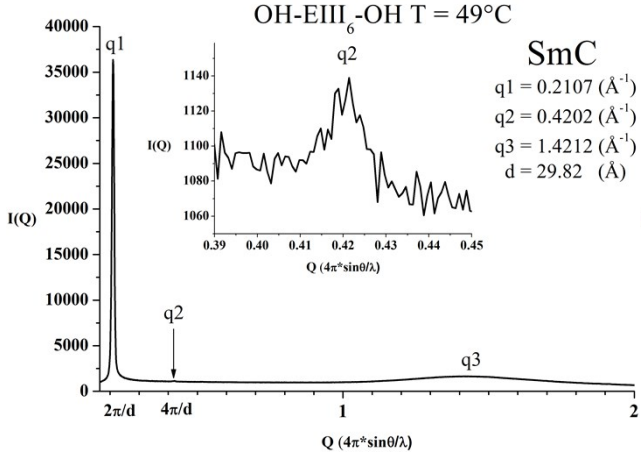

OH-EIII$_6$-OH T = RT

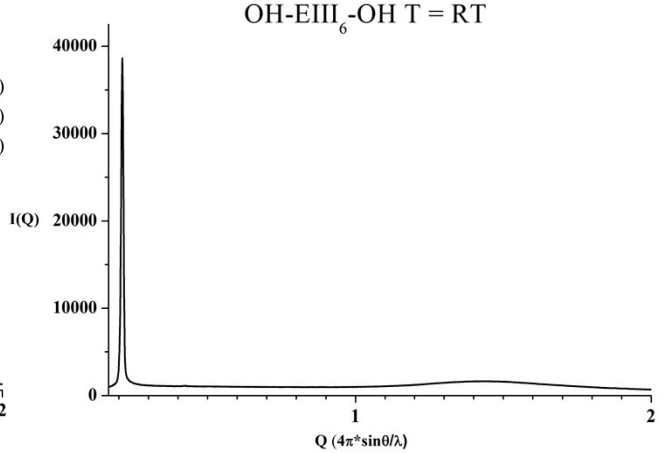

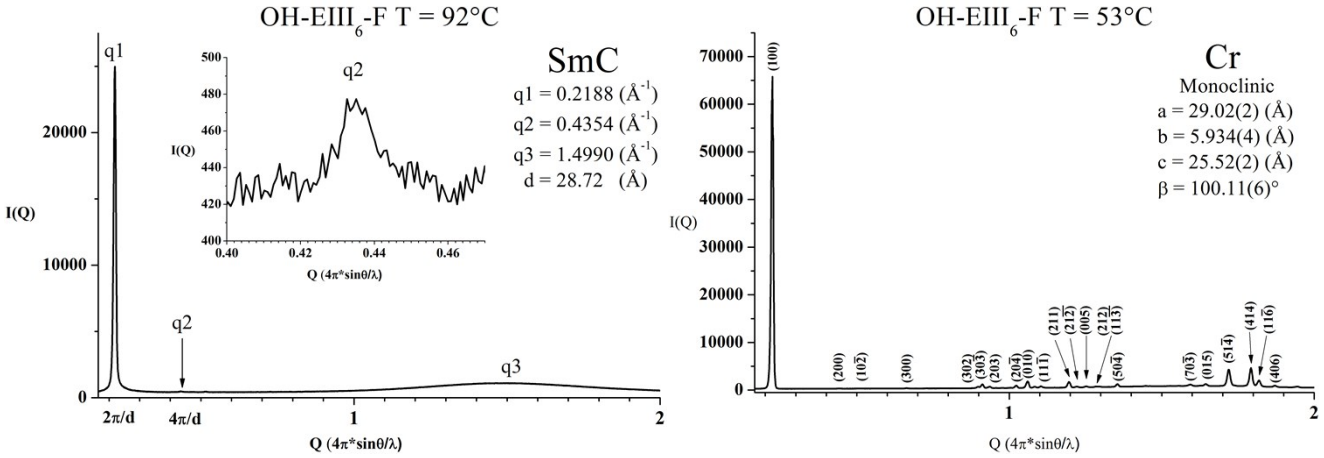

Figure S8 The variable – temperature XRD measurements for Schiff base mesogens.

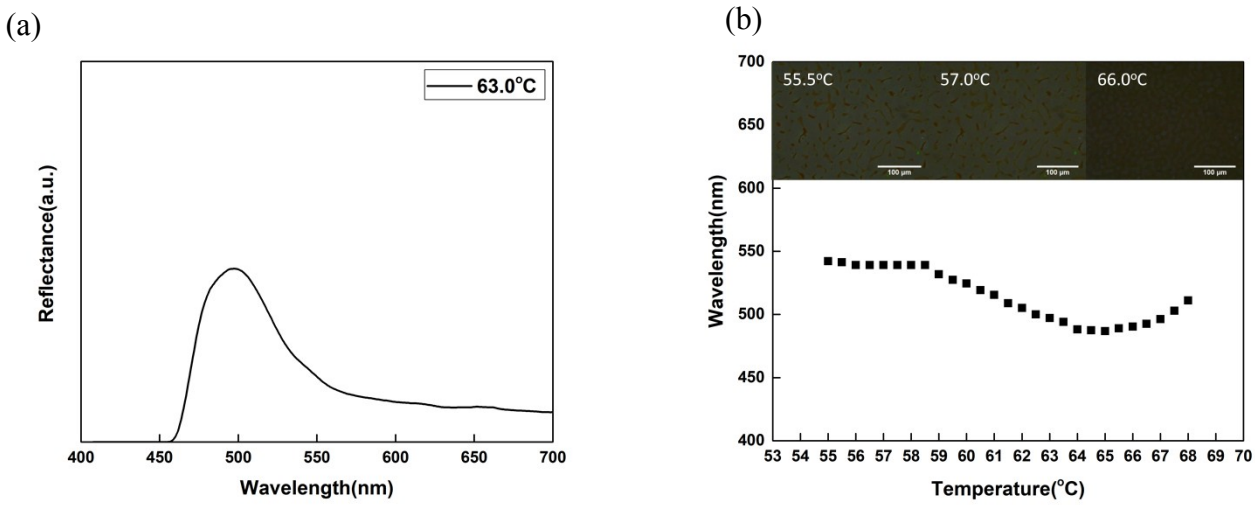

Figure S9 (a) A typical shape of the reflection spectrum (b) The temperature dependence of the Bragg reflection wavelength for the blending mixture consisting of **H-EI$_6$-F** + 30% **S811** at cooling rate with 0.2 °C min^{-1}. The inset shows the POM image of BPs at different temperature.

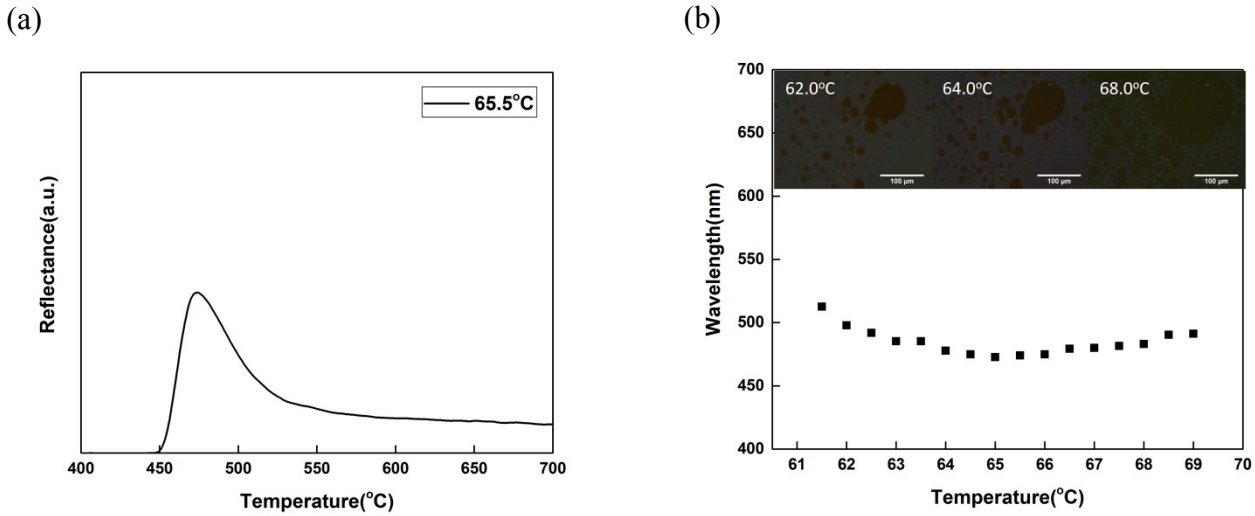

Figure S10 (a) Temperature dependence of typical reflectance profile (b) The temperature dependence of the Bragg reflection wavelength for the blending mixture consisting of **H-EI$_6$-F** + 30% **S811** at a heating rate with 0.2 °C min^{-1}. The inset shows the POM image of BPs at different temperature.

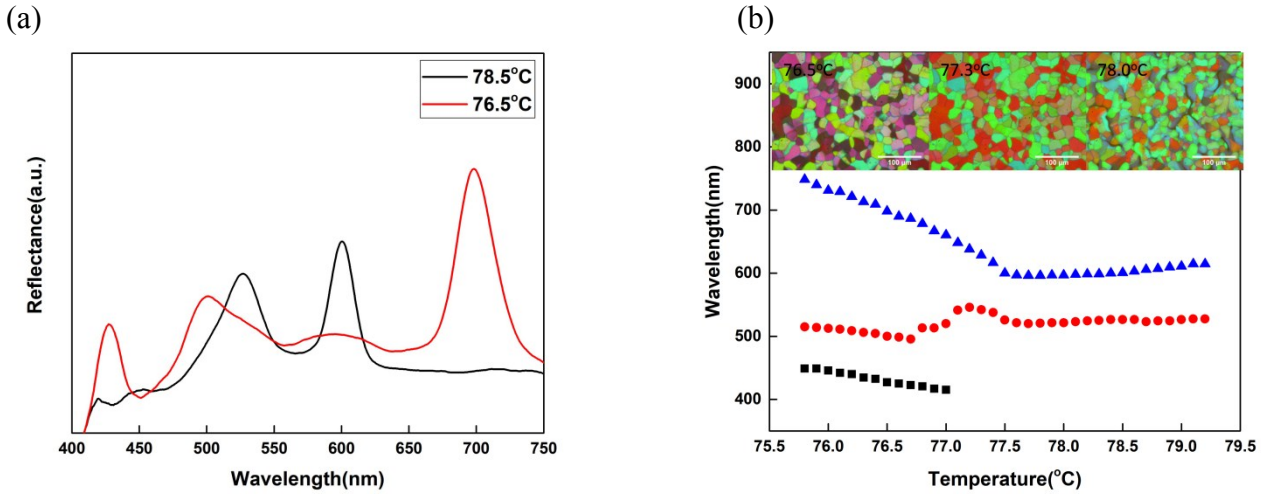

Figure S11 (a) typical shapes of the reflection spectra (b) The temperature dependence of the Bragg reflection wavelength for the blending mixture consisting of **OH-EI$_6$-OH** + 25% **S811** at a cooling rate with 0.2 °C min^{-1}. The inset shows the POM image of BPs at different temperature.

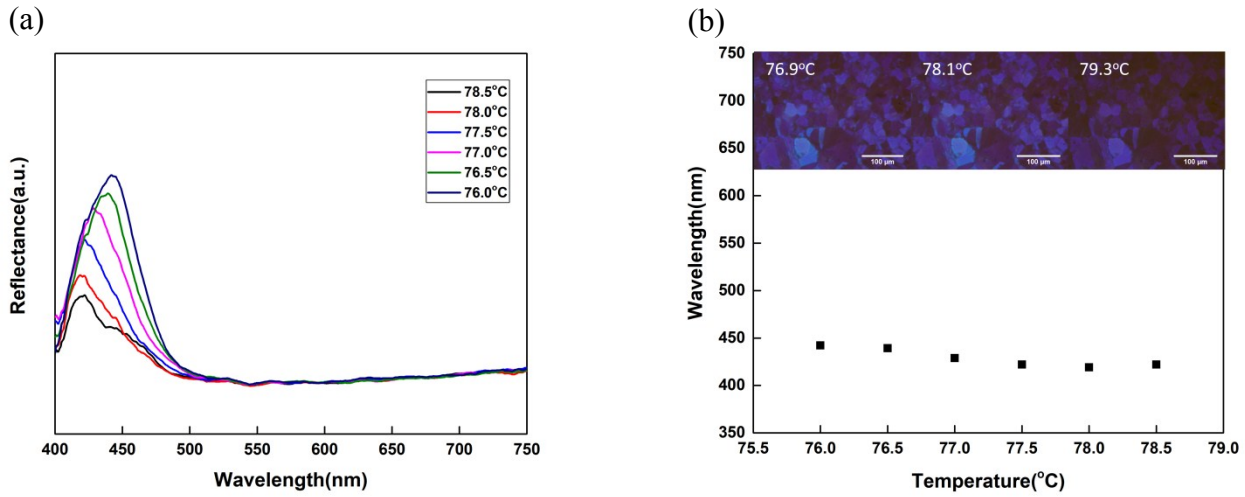

Figure S12 (a) Temperature dependence of typical reflectance profile (b) The temperature dependence of the Bragg reflection wavelength for the blending mixture consisting of **H-EI$_6$-OH** + 10% **ISO(6OBA)$_2$** at a heating rate with 0.2 °C min^{-1}. The inset shows the POM image of BPs at different temperature.

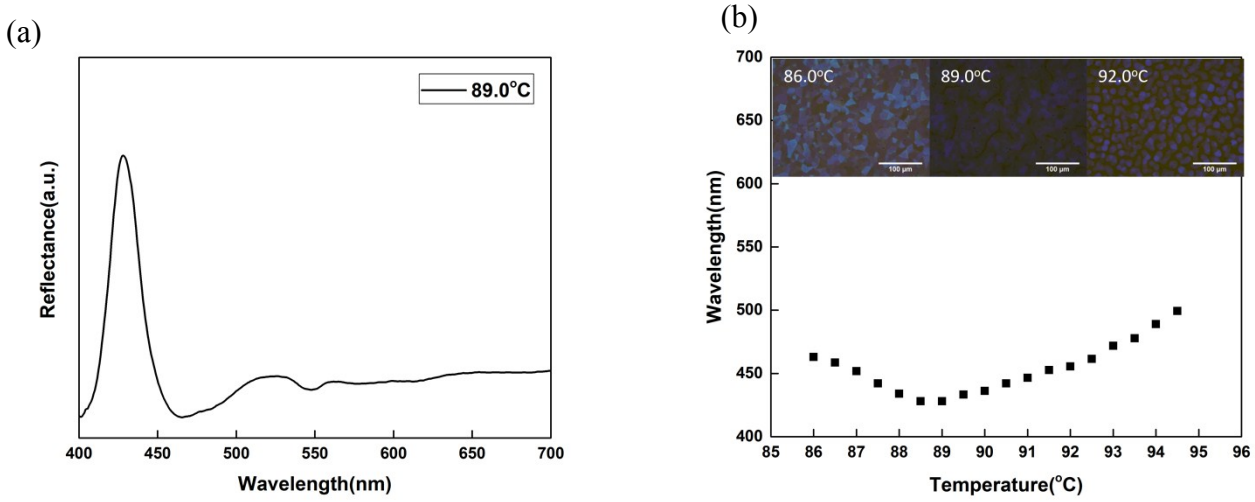

Figure S13 (a) Temperature dependence of typical reflectance profile (b) The temperature dependence of the Bragg reflection wavelength for the blending mixture consisting of **OH-EI$_6$-OH** + 10% **ISO(6OBA)$_2$** at a cooling rate with 0.2 °C min^{-1}. The inset shows the POM image of BPs at different temperature.

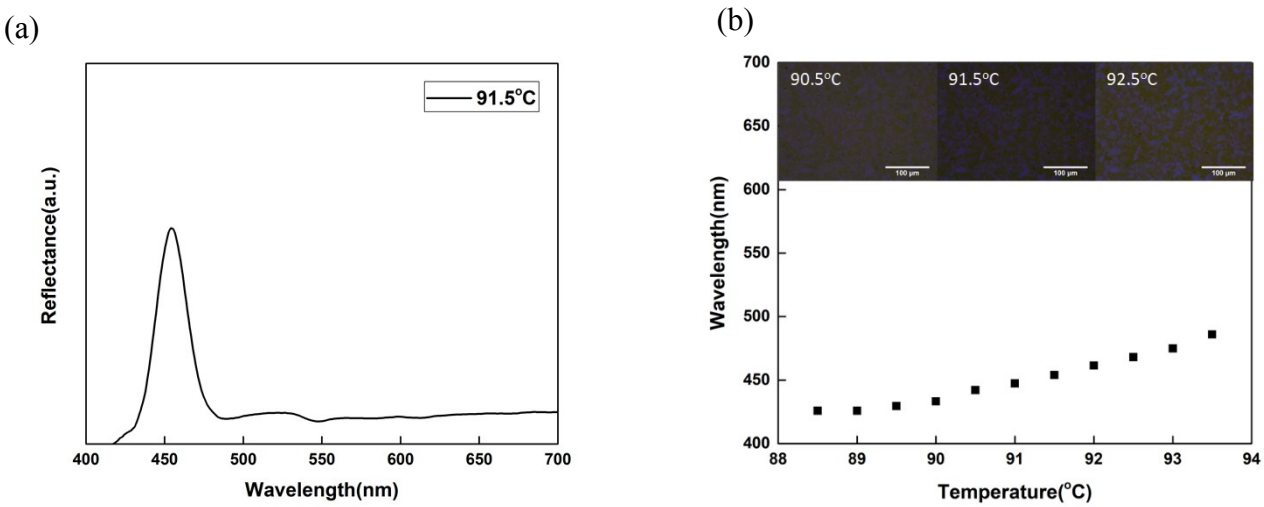

Figure S14 (a) Temperature dependence of typical reflectance profile (b) The temperature dependence of the Bragg reflection wavelength for the blending mixture consisting of **OH-EI$_6$-OH** + 10% **ISO(6OBA)$_2$** at a heating rate of 0.2 °C min^{-1}. The inset shows the POM image of BPs at different temperature.

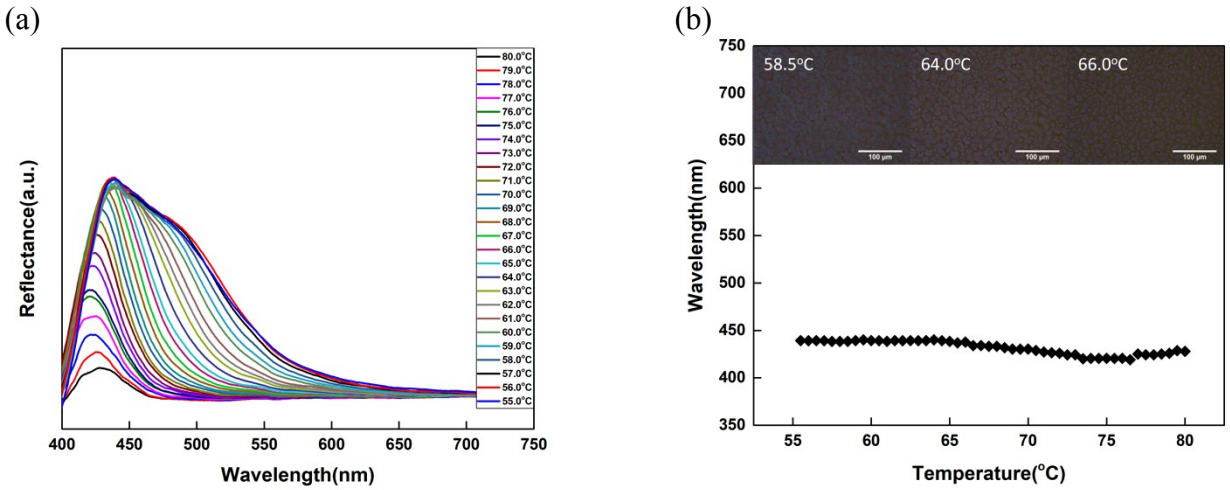

Figure S15 (a) Temperature dependence of typical reflectance profile (b) The temperature dependence of the Bragg reflection wavelength for the blending mixture consisting of **H-EI$_6$-F** + 10% **ISO(6OBA)$_2$** at a cooling rate with 0.2 °C min^{-1}. The inset shows the POM image of BPs at different temperature.

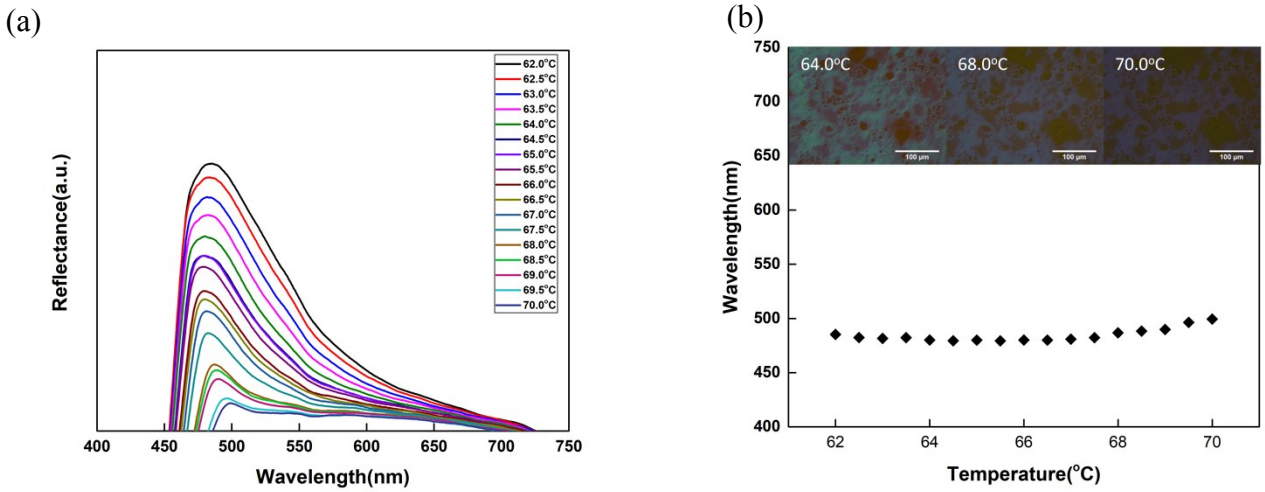

Figure S16 (a) Temperature dependence of typical reflectance profile (b) The temperature dependence of the Bragg reflection wavelength for the blending mixture consisting of **H-EI$_6$-F** + 10% **ISO(6OBA)$_2$** at a heating with 0.2 °C min^{-1}. The inset shows the POM image of BPs at different temperature.

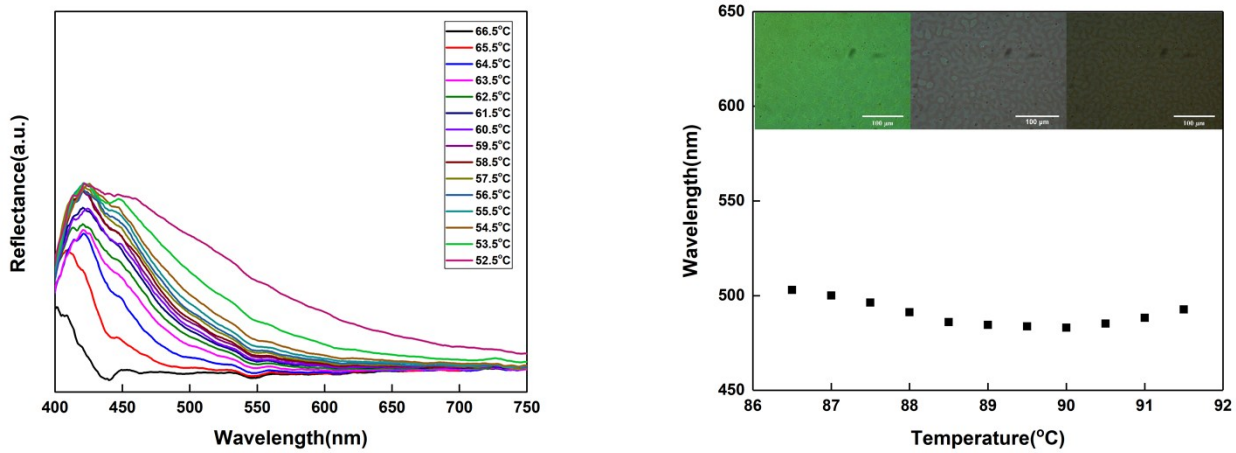

Figure S17 (a) Temperature dependence of typical reflectance profile (b) The temperature dependence of the Bragg reflection wavelength for the blending mixture consisting of **H-EIII$_6$** + 40% **S811** at a cooling rate with 0.2 °C min^{-1}. The inset shows the POM image of BPs at different temperature.

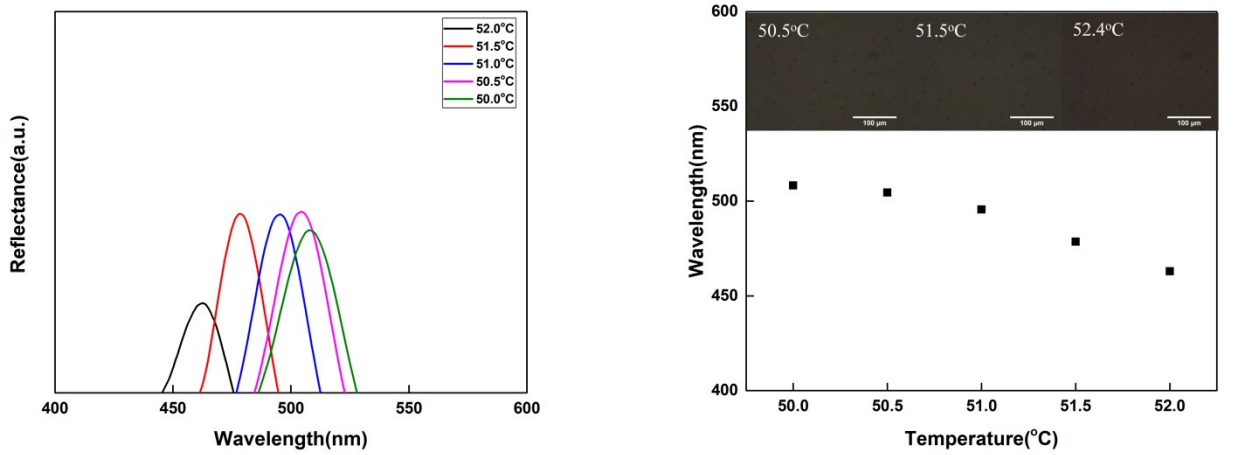

Figure S18 (a) Temperature dependence of typical reflectance profile (b) The temperature dependence of the Bragg reflection wavelength for the blending mixture consisting of **H-EIII$_6$-OH** + 30% **S811** at a cooling rate with 0.2 °C min^{-1}. The inset shows the POM image of BPs at different temperature.

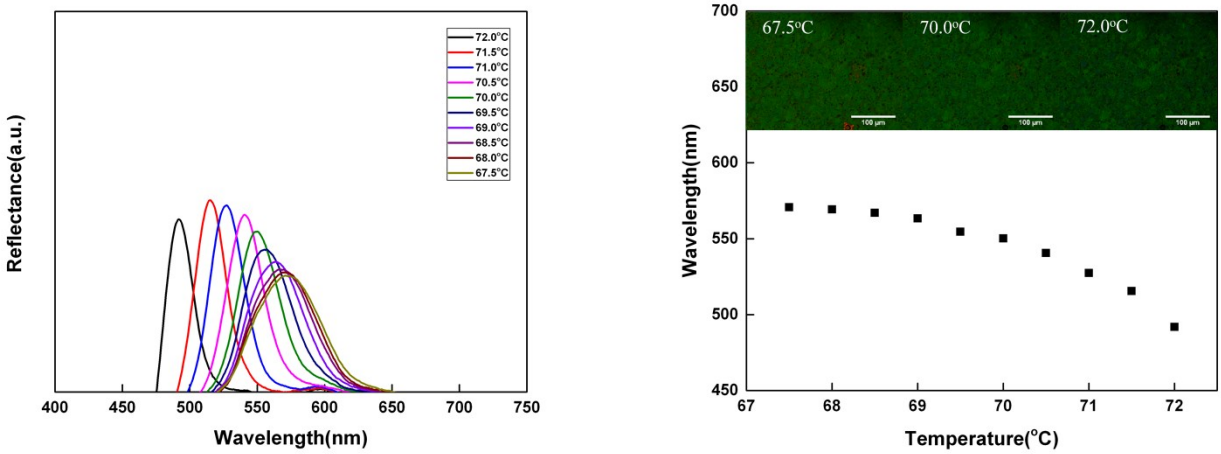

Figure S19 (a) Temperature dependence of typical reflectance profile (b) The temperature dependence of the Bragg reflection wavelength for the blending mixture consisting of **OH-EIII$_6$-OH** + 25% **S811** at a cooling rate with 0.2 °C min^{-1}. The inset shows the POM image of BPs at different temperature.

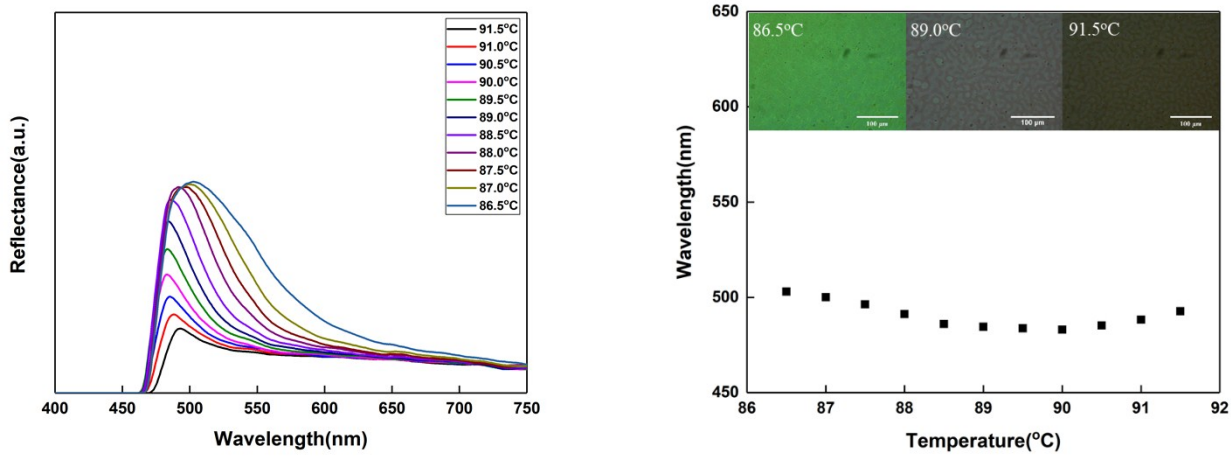

Figure S20 (a) Temperature dependence of typical reflectance profile (b) The temperature dependence of the Bragg reflection wavelength for the blending mixture consisting of **OH-EIII$_6$-F** + 30% **S811** at a cooling with 0.2 °C min^{-1}. The inset shows the POM image of BPs at different temperature.

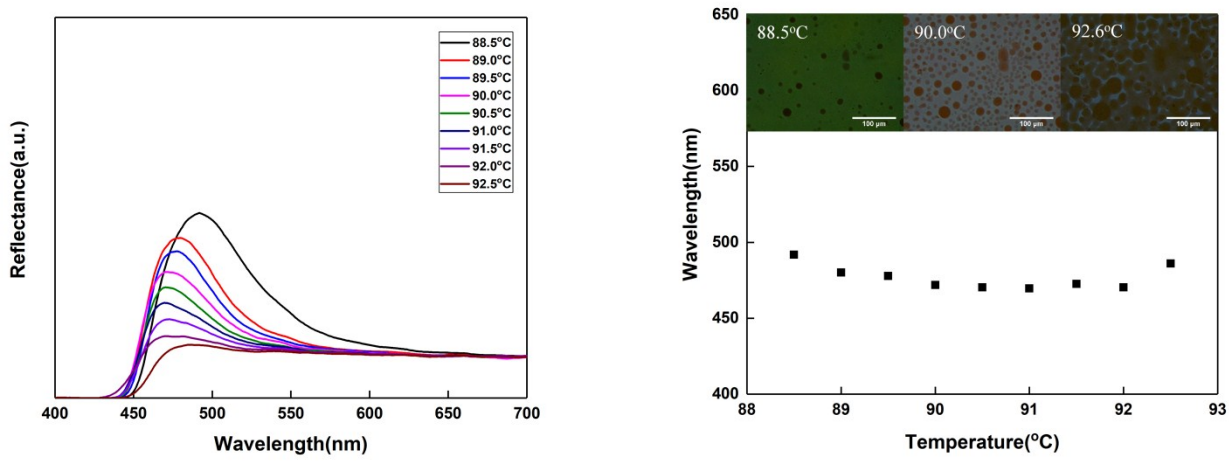

Figure S21 (a) Temperature dependence of typical reflectance profile (b) The temperature dependence of the Bragg reflection wavelength for the blending mixture consisting of **OH-EIII$_6$-F** + 30% **S811** at a heating rate with 0.2 °C min^{-1}. The inset shows the POM image of BPs at different temperature.

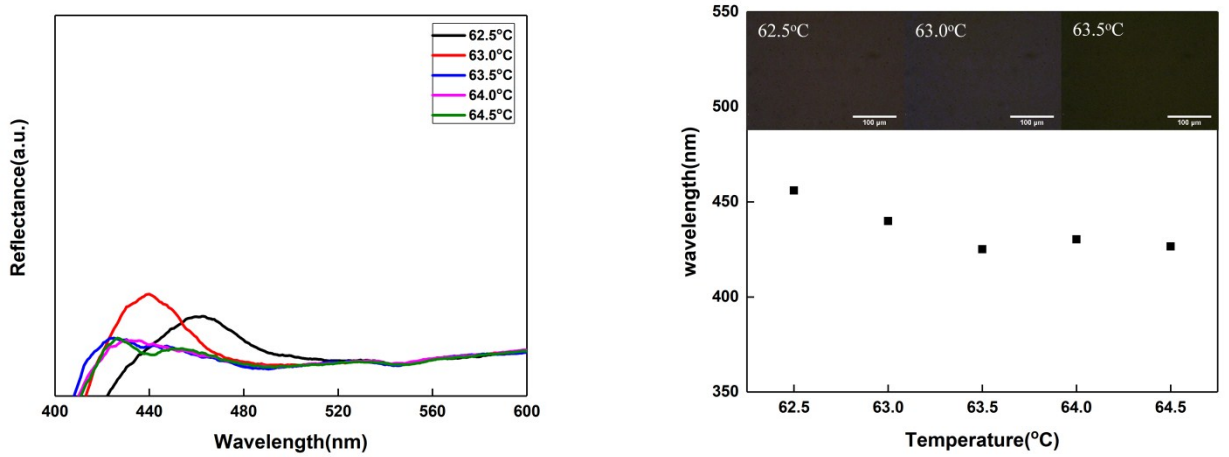

Figure S22 (a) Temperature dependence of typical reflectance profile (b) The temperature dependence of the Bragg reflection wavelength for the blending mixture consisting of **H-EIII$_6$-F** + 35% **S811** at a heating rate with 0.2 °C min^{-1}. The inset shows the POM image of BPs at different temperature.

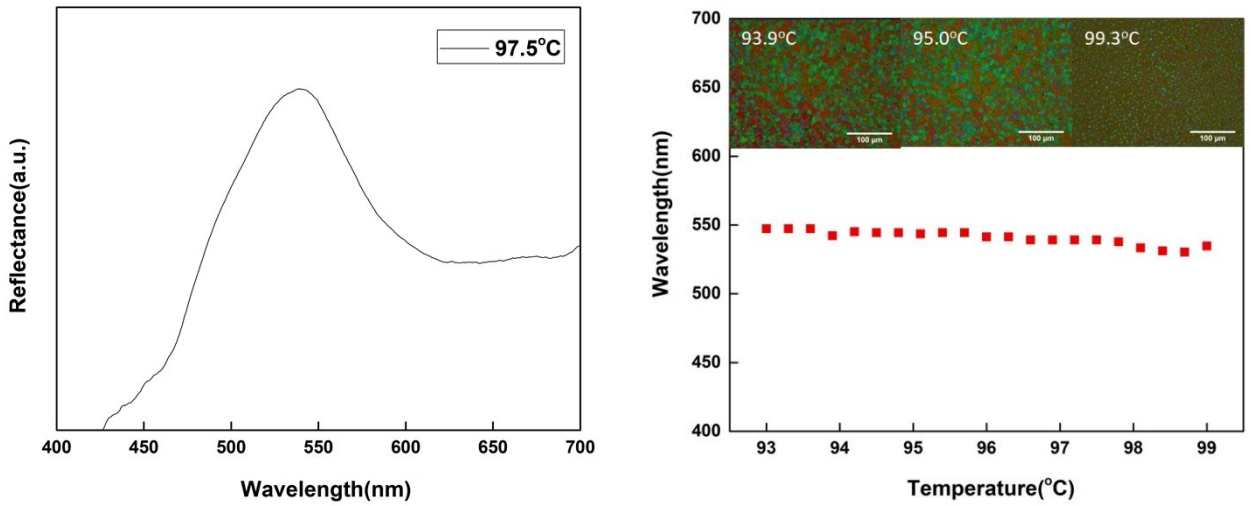

Figure S23 (a) Temperature dependence of typical reflectance profile (b) The temperature dependence of the Bragg reflection wavelength for the blending mixture consisting of **OH-EIII$_6$-OH** + 5% **ISO(6OBA)$_2$** at a cooling rate with 0.2 °C min^{-1}. The inset shows the POM image of BPs at different temperature.

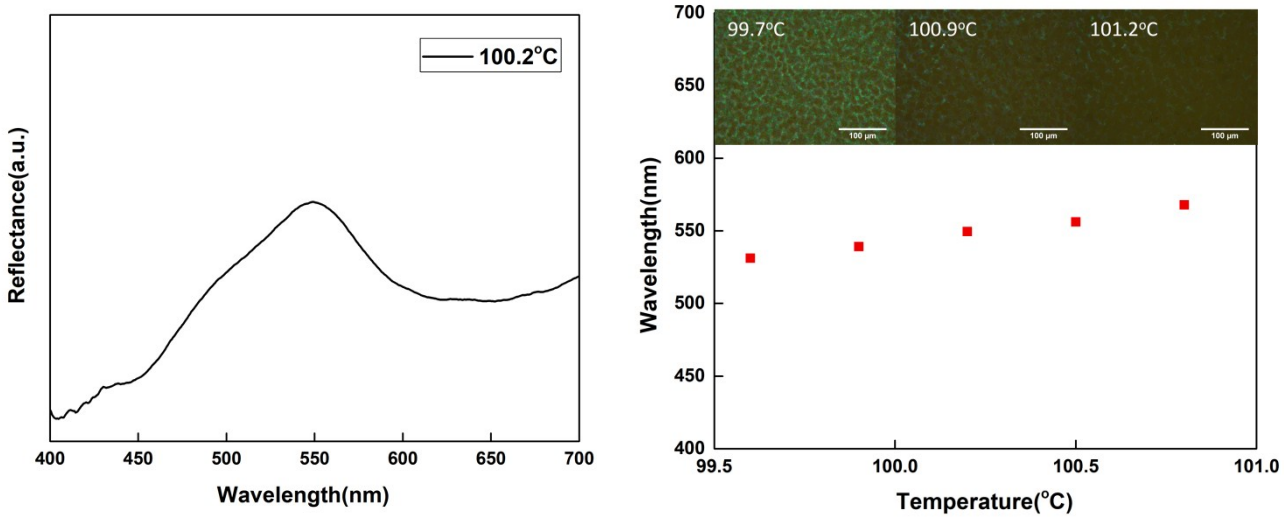

Figure S24 (a) Temperature dependence of typical reflectance profile (b) The temperature dependence of the Bragg reflection wavelength for the blending mixture consisting of **OH-EIII$_6$-OH** + 5% **ISO(6OBA)$_2$** at a heating rate with 0.2 °C min^{-1}. The inset shows the POM image of BPs at different temperature.

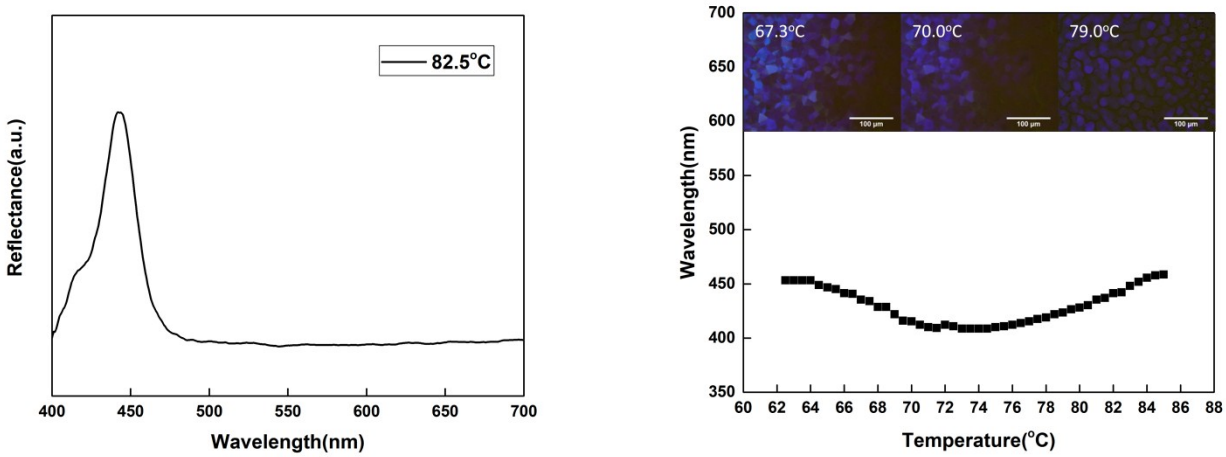

Figure S25 (a) Temperature dependence of typical reflectance profile (b) The temperature dependence of the Bragg reflection wavelength for the blending mixture consisting of **H-EIII$_6$-F** + 15% **ISO(6OBA)$_2$** at a cooling rate with 0.2 °C min^{-1}. The inset shows the POM image of BPs at different temperature.

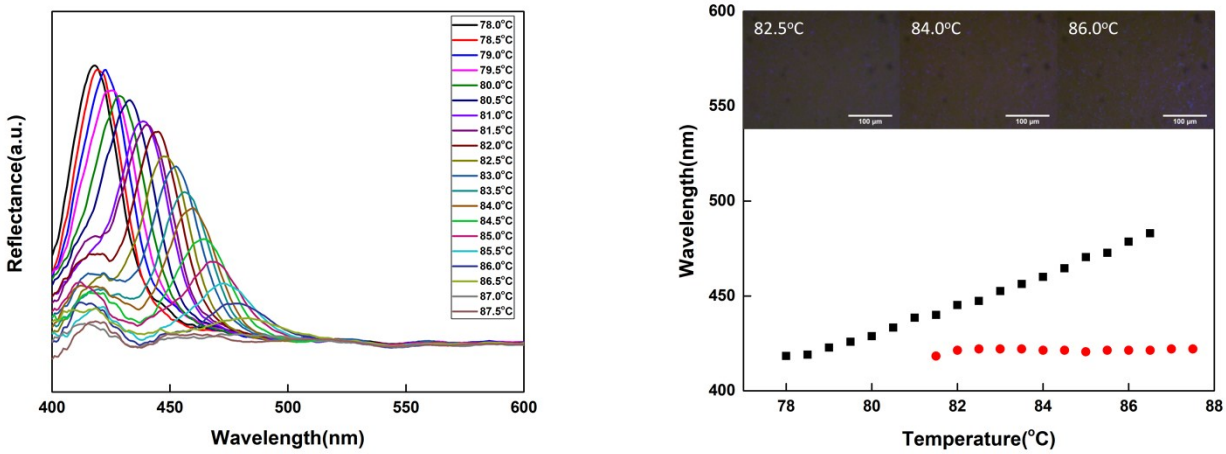

Figure S26 (a) Temperature dependence of typical reflectance profile (b) The temperature dependence of the Bragg reflection wavelength for the blending mixture consisting of **H-EIII$_6$-F** + 15% **ISO(6OBA)$_2$** at a heating rate with 0.2 °C min^{-1}. The inset shows the POM image of BPs at different temperature.

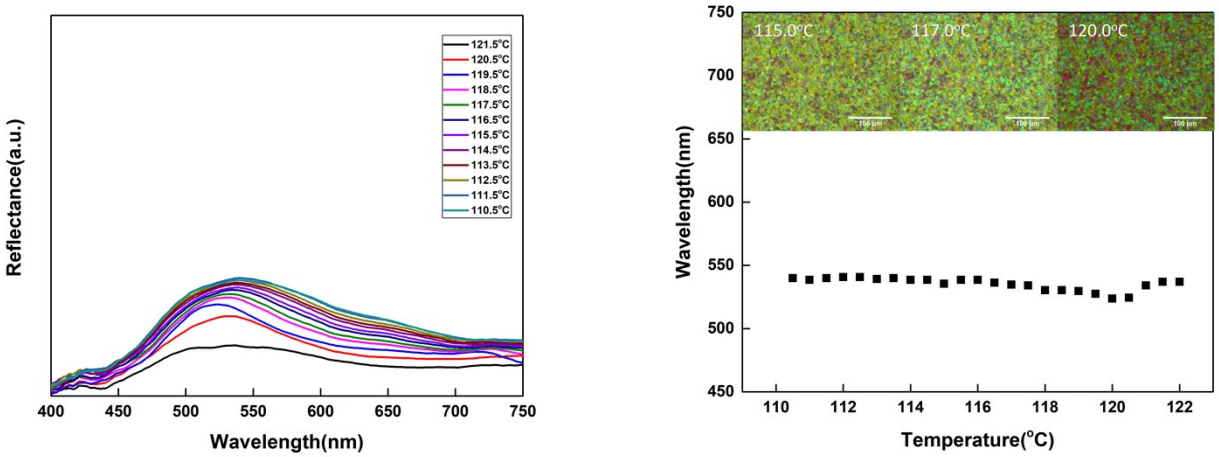

Figure S27 (a) Temperature dependence of typical reflectance profile (b) The temperature dependence of the Bragg reflection wavelength for the blending mixture consisting of **OH-EIII$_6$-F** + 10% **ISO(6OBA)$_2$** at a cooling rate with 0.2 °C min^{-1}. The inset shows the POM image of BPs at different temperature.

HOMO

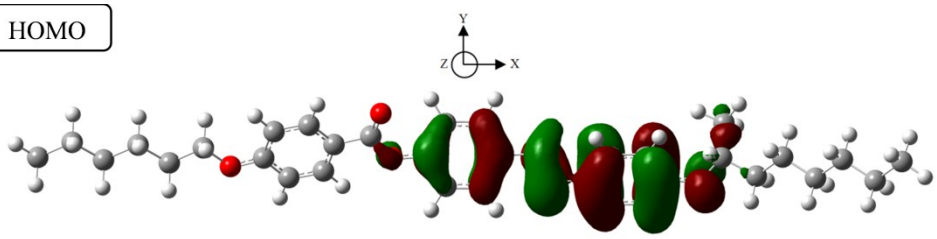

LUMO

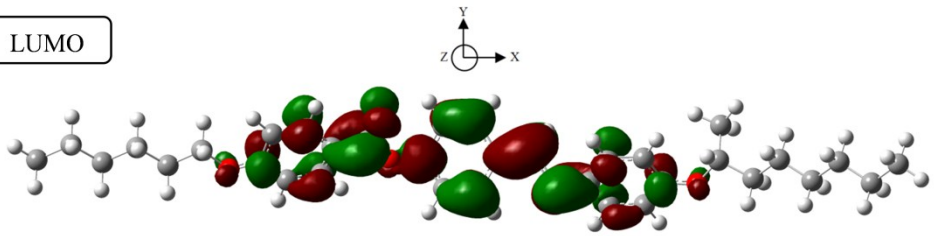

H-EI$_6$

HOMO

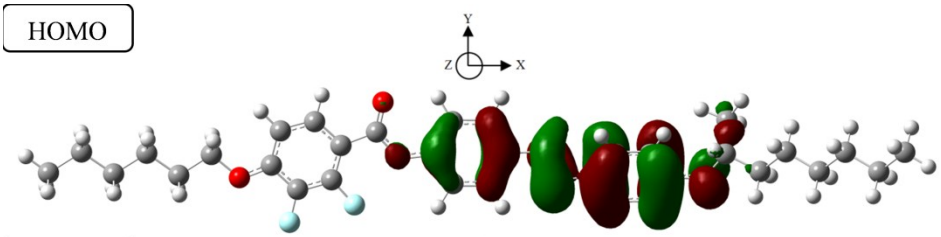

LUMO

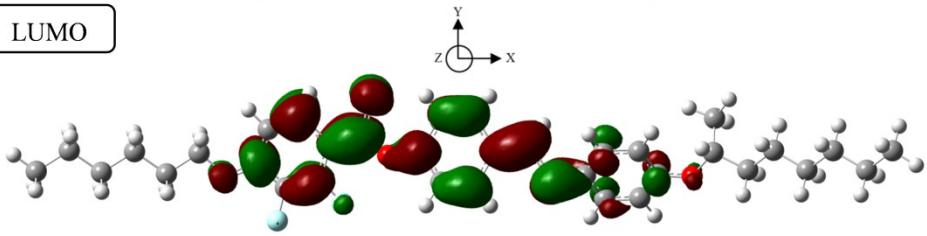

H-EI$_6$-F

HOMO

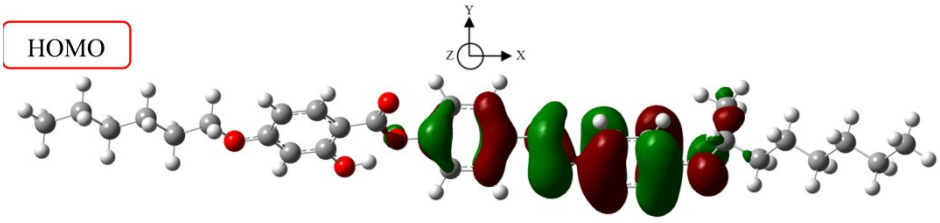

LUMO

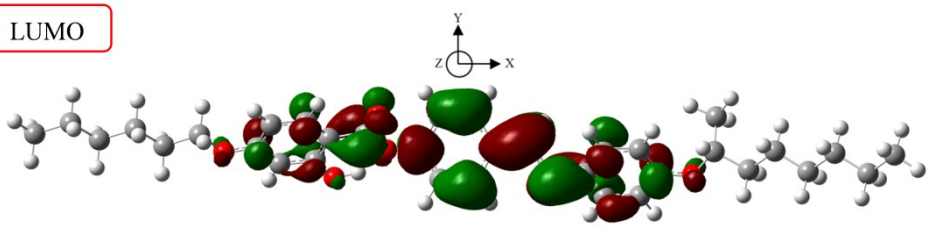

H-EI$_6$-OH

HOMO

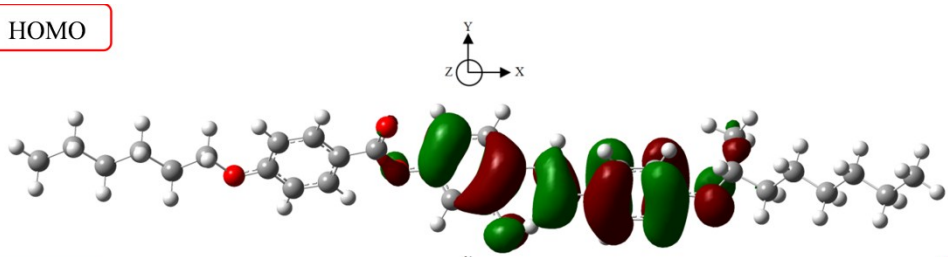

LUMO

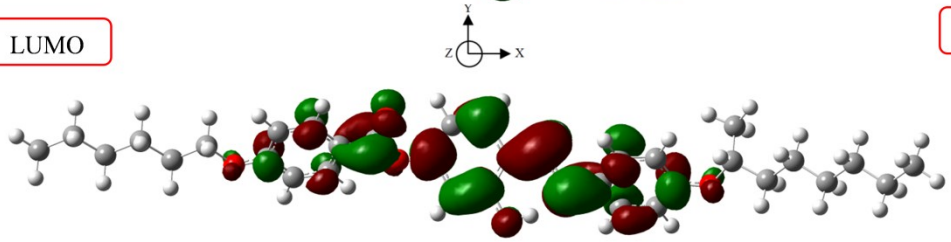

OH-EI$_6$

HOMO

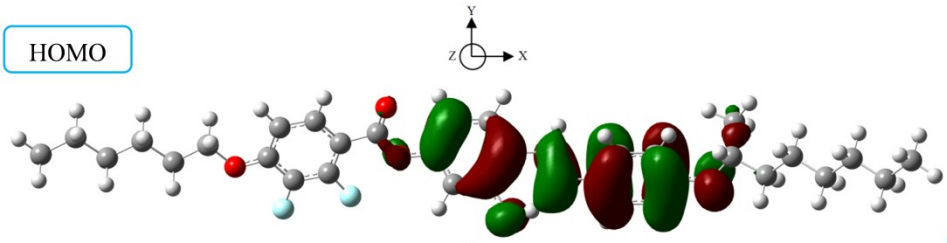

OH-EI$_6$-F

LUMO

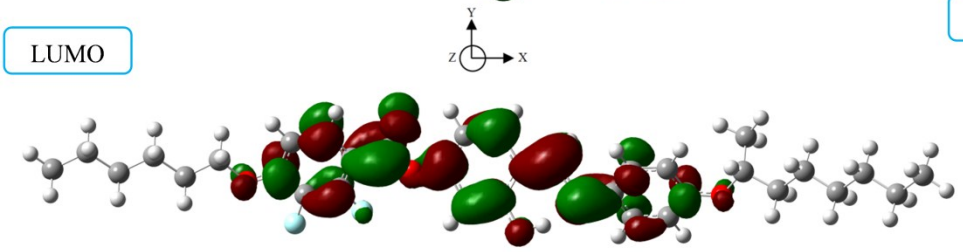

HOMO

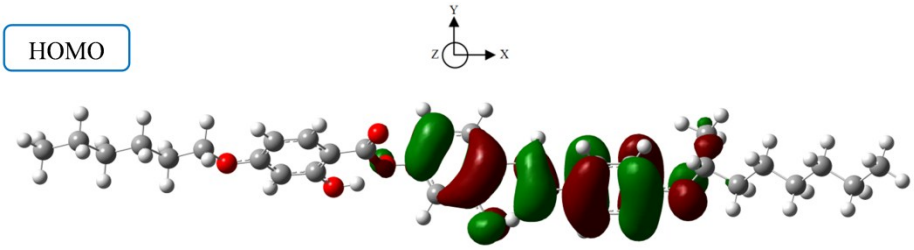

OH-EI$_6$-OH

LUMO

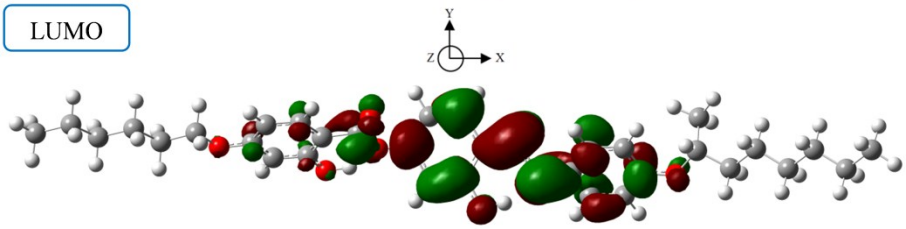

HOMO

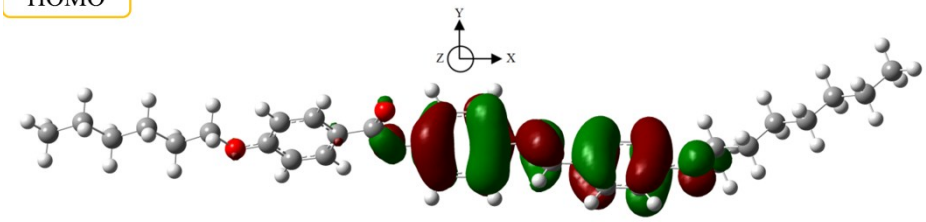

H-EIII$_6$

LUMO

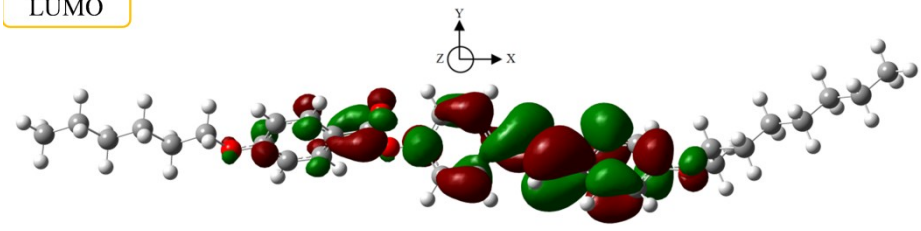

HOMO

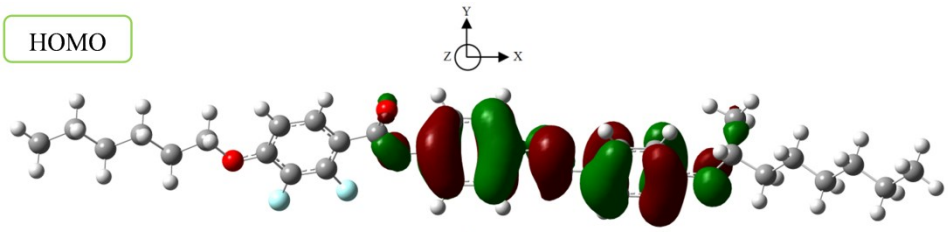

LUMO

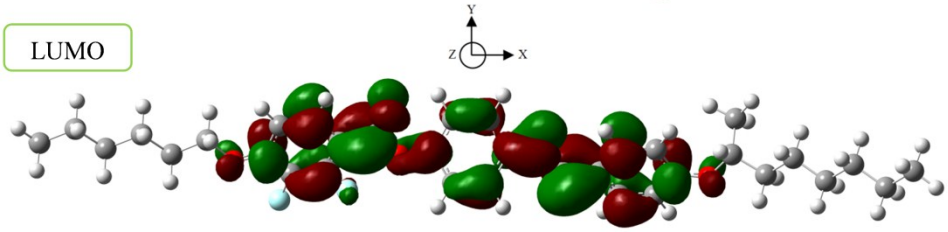

H-EIII$_6$-F

HOMO

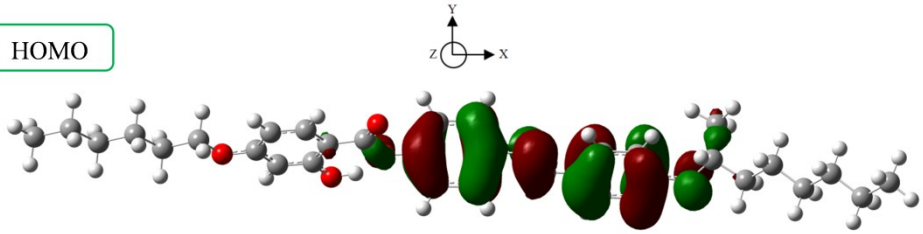

LUMO

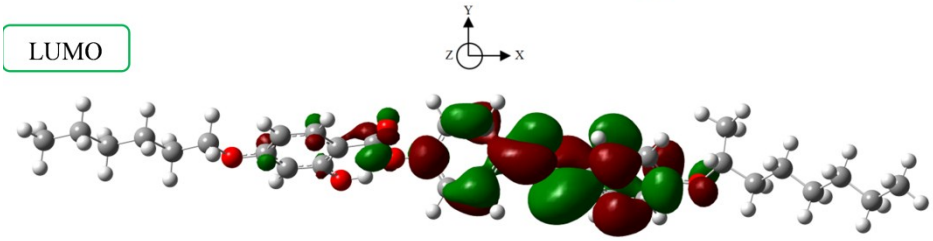

H-EIII$_6$-OH

HOMO

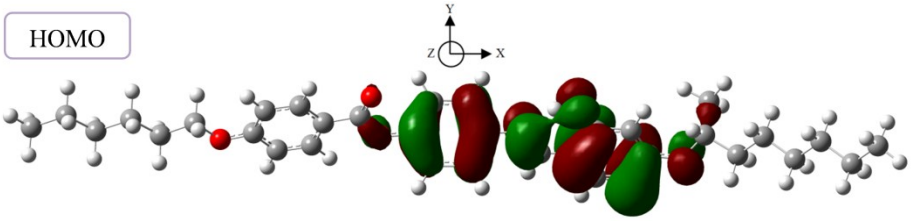

LUMO

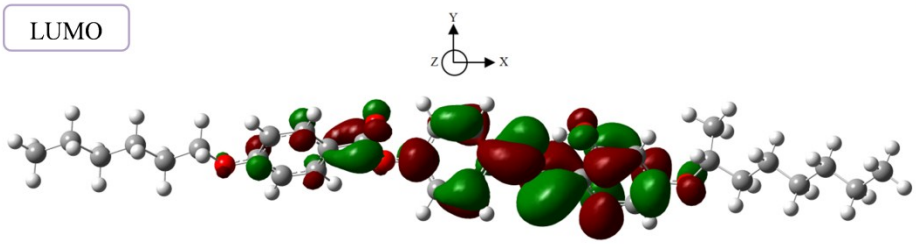

OH-EIII$_6$

HOMO

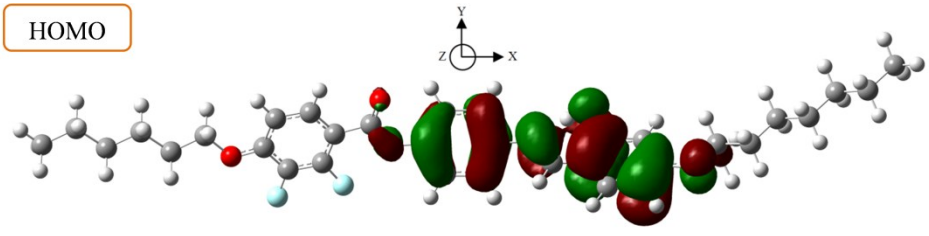

LUMO

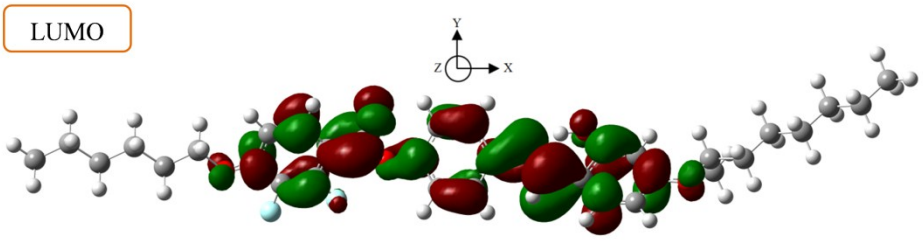

OH-EIII$_6$-F

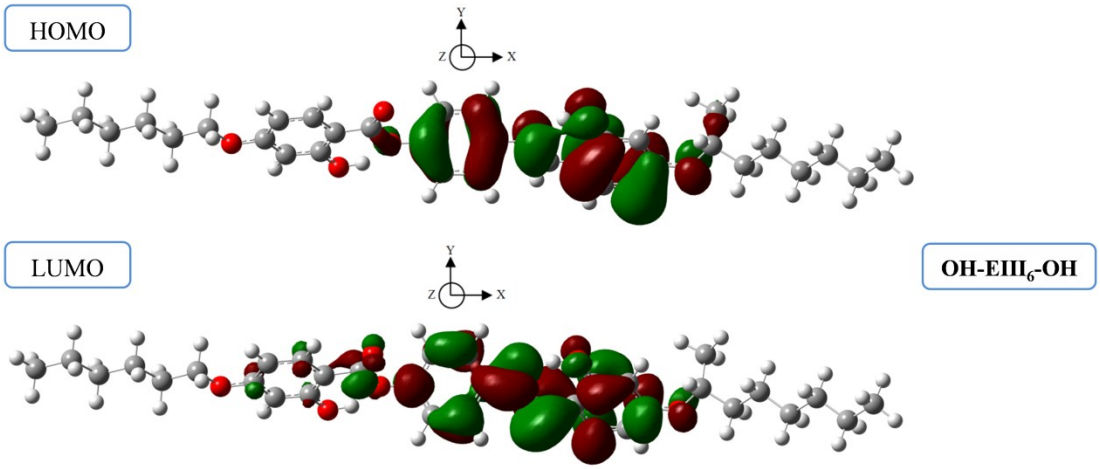

Figure S28 The HOMO and LUMO of Schiff base mesogens. The simulation exchange functional and basis set are CAM-B3LYP and 6-311G(d, p), respectively. The isosurface is drawn at value of 0.02

Table S1 DFT calculated HOMO, LUMO, energy gap, dipole moment components, μ_x, μ_y, μ_z and modulus (μ) for Schiff base compounds.

Compound	Energy (eV)			Dipole moment (m in Debye)			
	HOMO	LUMO	ΔE (eV)	μ_x	μ_y	μ_z	μ_{total}
H-EI$_6$	-6.8868	-0.4414	6.4455	-2.4496	1.5921	0.4135	2.9506
H-EI$_6$-F	-6.8945	-0.6230	6.2716	-2.8581	3.4159	1.0496	4.5759
H-EI$_6$-OH	-6.9982	-0.5544	6.4438	-0.4046	2.4468	1.2990	2.7996
OH-EI$_6$	-6.9897	-0.5385	6.4512	-0.6128	2.5888	0.2704	2.6740
OH-EI$_6$-F	-7.0131	-0.6492	6.3639	-0.8568	4.3000	1.6678	4.6911
OH-EI$_6$-OH	-7.1194	-0.6621	6.4573	1.5361	3.2433	1.3477	3.8334
H-EIII$_6$	-7.0681	-0.2717	6.7964	-0.2101	-0.4969	-0.3511	0.6437
H-EIII$_6$-F	-7.0878	-0.3714	6.7163	-0.4044	1.1104	1.0407	1.5747
H-EIII$_6$-OH	-7.2312	-0.3808	6.8504	1.8446	0.0364	0.4509	1.8993
OH-EIII$_6$	-7.0199	-0.4122	6.6077	-1.9845	-1.1800	-0.9176	2.4845
OH-EIII$_6$-F	-7.0335	-0.5120	6.5215	-2.2041	0.5523	1.5859	2.7710
OH-EIII$_6$-OH	-7.1542	-0.5178	6.6364	0.0836	-0.4762	-0.0917	0.4921

Table S2 DFT calculated principal polarizability components relative to the molecular polarizability tensor α.

Compound	α_{XX}	α_{YY}	α_{ZZ}	$\alpha^{iso\ a}$	$\Delta\alpha^b$	$\eta_\alpha{}^c$
H-EI$_6$	739.467	326.712	271.340	445.84	440.441	0.1886
H-EI$_6$-F	746.865	346.633	250.753	448.08	448.172	0.3209
H-EI$_6$-OH	747.370	321.134	283.699	450.73	444.954	0.1262
OH-EI$_6$	772.080	341.410	283.157	465.55	459.797	0.1900
OH-EI$_6$-F	755.558	340.866	265.018	453.81	452.616	0.2514
OH-EI$_6$-OH	760.645	323.600	289.204	457.82	454.243	0.1136
H-EIII$_6$	734.196	313.275	284.577	444.02	435.270	0.0989
H-EIII$_6$-F	736.729	323.101	275.726	445.19	437.316	0.1625
H-EIII$_6$-OH	741.431	308.936	298.096	449.49	437.915	0.0371
OH-EIII$_6$	754.362	319.831	284.977	453.06	451.958	0.1157
OH-EIII$_6$-F	759.949	333.978	269.383	454.44	458.269	0.2114
OH-EIII$_6$-OH	763.198	316.319	295.868	458.46	457.105	0.0671

a: isotropic component, $\alpha^{iso} = (\alpha_{XX}+\alpha_{YY}+\alpha_{ZZ})/3$

b: polarizability anisotropy, $\Delta\alpha = [\alpha_{XX} - (\alpha_{YY+}\ \alpha_{ZZ})/2]$

c: asymmetry parameter, $\eta_\alpha = [(\alpha_{YY}-\alpha_{ZZ})/(\alpha_{XX}-\alpha^{iso})]$